Determining stoichiometry and kinetics of two thermophilic nitrifying communities as a crucial step in the development of thermophilic nitrogen removal

Determining stoichiometry and kinetics of two thermophilic nitrifying communities as a crucial step in the development of thermophilic nitrogen removal

Tom G.L. Vandekerckhove[1], Frederiek-Maarten Kerckhof[1], Chaïm De Mulder[2], Siegfried E. Vlaeminck[1,3*], Nico Boon[1*]✉

[1] Center for Microbial Ecology and Technology (CMET), Ghent University, Coupure Links 653, 9000 Gent, Belgium

[2] BIOMATH, Department of Mathematical Modelling, Statistics and Bioinformatics, Ghent University, Coupure Links 653, 9000 Gent, Belgium

[3] Research Group of Sustainable Energy, Air and Water Technology, University of Antwerp, Groenenborgerlaan 171, 2020 Antwerpen, Belgium

*These authors contributed equally and are both senior authors for this work

✉ Corresponding author: Nico.boon@ugent.be

Abstract

Nitrification and denitrification, the key biological processes for thermophilic nitrogen removal, have separately been established in bioreactors at 50°C. A well-characterized set of kinetic parameters is essential to integrate these processes while safeguarding the autotrophs performing nitrification. Knowledge on thermophilic nitrifying kinetics is restricted to isolated or highly enriched batch cultures, which do not represent bioreactor conditions. This study characterized the stoichiometry and kinetics of two thermophilic (50°C) nitrifying communities. The most abundant ammonia oxidizing archaea (AOA) were related to the *Nitrososphaera* genus, clustering relatively far from known species *Nitrososphaera gargensis* (95.5% 16S rRNA gene sequence identity). The most abundant nitrite oxidizing bacteria (NOB) were related to *Nitrospira calida* (97% 16S rRNA gene sequence identity). The nitrification biomass yield was 0.20-0.24 g VSS g^{-1} N, resulting mainly from a high AOA yield (0.16-0.20 g VSS g^{-1} N), which was reflected in a high AOA abundance in the community (57-76%) compared to NOB (5-11%). Batch-wise determination of decay rates (AOA: 0.23-0.29 d^{-1}; NOB: 0.32-0.43 d^{-1}) rendered an overestimation compared to *in situ* estimations of overall decay rate (0.026-0.078 d^{-1}). Possibly, the inactivation rate rather than the actual decay rate was determined in batch experiments. Maximum growth rates of AOA and NOB were 0.12-0.15 d^{-1} and 0.13-0.33 d^{-1} respectively. NOB were susceptible to nitrite, opening up opportunities for shortcut nitrogen removal. However, NOB had a similar growth rate and oxygen affinity (0.15-0.55 mg O_2 L^{-1}) as AOA and were resilient towards free ammonia (IC_{50} >16 mg NH_3-N L^{-1}). This might complicate NOB outselection using common practices to establish shortcut nitrogen removal (SRT control; aeration control; free ammonia shocks). Overall, the obtained insights can assist in integrating thermophilic conversions and facilitate single-sludge nitrification/denitrification.

Keywords: biological nitrogen removal; *Nitrososphaera*; *Nitrospira*; substrate affinity; Archaea

1. Introduction

The discharge of wastewater contributes significantly to the accumulation of reactive nitrogen species, (Coppens et al., 2016), which can elicit major environmental burdens in receiving water bodies, including eutrophication and fish mortality (Camargo and Alonso, 2006). Biological nitrogen removal is applied to convert toxic ammonia to harmless nitrogen gas and is usually operated at temperatures between 5 and 35°C (Henze et al., 2008). Thermophilic treatment might be a viable alternative for specific applications, such as warm wastewaters or industries with excess heat available. Thermophilic aerobic carbon removal has been extensively reviewed and is reported to be more stable, with a higher level of decontamination and lower production of biological sludge when compared to mesophilic treatment (Lapara and Alleman, 1999). Thermophilic denitrification was found to be fast in start-up (< 1 week), accompanied by improved settling, reduced carbon requirement and lower sludge production (Courtens et al., 2014b). To compose an integrated treatment solution for nitrogen, the development of thermophilic nitrification is essential.

Thermophilic ammonia oxidation in nature is mainly an archaeal feature so far. Only some ammonia oxidizing bacteria (AOB), representatives of the *Nitrosomonas* genus and some unknown ammonia oxidizing bacteria, have been reported to grow optimally up to 46-50°C (Lebedeva et al., 2005). On the other hand, thermophilic ammonia oxidizing archaea (AOA) were widely found using the ammonia monooxygenase subunit A (*amoA*) in deep-sea hydrothermal vents (Baker et al., 2012, Wang et al., 2009), subsurface thermal springs (Spear et al., 2007, Weidler et al., 2008), terrestrial hot springs (Dodsworth et al., 2011, Reigstad et al., 2008) and composting facilities (Zeng et al., 2011). Besides the genomic detection, some representatives with an optimum temperature >45°C have been isolated and described, namely *Candidatus Nitrosocaldus yellowstonii*, *Candidatus Nitrososphaera gargensis*, *Candidatus Nitrosotenius uzonensis* and *Candidatus Nitrosocaldus islandicus* (Daebeler et

al., 2017, de la Torre et al., 2008, Hatzenpichler et al., 2008, Lebedeva et al., 2013). The apparent dominion of AOA over AOB at high temperatures is likely related to a higher substrate affinity and the oligotrophic nature of most natural habitats investigated (Martens-Habbena et al., 2009). In addition, AOA are distinguished from AOB by robust monolayer membranes with ether bound isoprenoid units, making them better equipped to survive extreme conditions compared to the bilayer membranes with ester bound fatty acid chains present in AOB (Schouten et al., 2013). As opposed to ammonia oxidation, thermophilic nitrite oxidation remains attributed to bacteria, with all detected or enriched cultures related to *Nitrospira calida* (Courtens et al., 2016a, Edwards et al., 2013, Lebedeva et al., 2011, Marks et al., 2012). One moderate thermophilic NOB related to the phylum *Chloroflexi Nitrolancea hollandica* was isolated and described as well (Sorokin et al., 2014).

To establish thermophilic nitrifying bioreactors, two distinct strategies were recently developed. A first strategy, called 'constant-temperature enrichment', involved the enrichment of a thermophilic compost-derived inoculum in a high-performing bioreactor at 50°C (Courtens et al., 2016a). Its time-consuming nature (350 days batch-wise enrichment; 560 days reactor enrichment) would impede the start-up of a full-scale wastewater treatment facility, being orders of magnitude larger than a lab-scale bioreactor. Upgrading existing mesophilic facilities using a temperature increase strategy may be more convenient. First attempts to use this strategy were unsuccessful to reach temperatures >45°C by using a stepwise increase higher than 2.5°C d^{-1} (Courtens et al., 2014a, Shore et al., 2012). The key to a successful upgrade was a gradual temperature increase of 0.08°C d^{-1}, providing sufficient time for a selection towards appropriate thermophiles (49.5°C) (Courtens et al., 2016b). Both strategies for the cultivation of thermophilic nitrifiers thus resulted in bioreactors with high nitrification rates. The thriving nitrifying communities consisted of *Nitrososphaera*

93 *gargensis*-related AOA and *Nitrospira calida*-related NOB, yet the respective functional
94 phylotypes of both reactors revealed distinctly different players (Courtens et al., 2016b).

95 The key biotechnological processes for nitrogen removal are at hand. The next step is to
96 conceive an efficient thermophilic nitrogen removal process by integrating heterotrophic
97 conversions with nitrification or nitritation. Compared to nitrifiers, heterotrophs are
98 characterized by a higher biomass yield (0.47 g VSS g^{-1} COD vs 0.17 g VSS g^{-1} N) and
99 growth rate (6 vs 0.8 d^{-1}) compared to nitrifiers (Henze et al., 2000). As the biomass
100 concentration in a treatment facility is usually fixed, changing organic loading rate relative to
101 the nitrogen load can result in excessive growth of heterotrophs, possibly lowering the sludge
102 retention time (SRT) below the nitrifier growth rate and, thus, resulting in the washout of
103 nitrifiers. To safely integrate these processes and set the boundaries safeguarding
104 nitrification, an elaborate set of kinetic parameters is essential. Knowledge on thermophilic
105 nitrifying kinetics is scarce and only available for isolated or highly enriched batch cultures,
106 which do not reproduce the conditions thriving in bioreactors. In this study, two thermophilic
107 nitrifying mixed cultures were kinetically and physiologically characterized. Furthermore,
108 full-length SMRT amplicon sequencing of the 16S rRNA gene (Pacific Biosciences Sequel
109 SMRT bell sequencing) allowed us to precisely determine the phylogeny of the different
110 thermophilic nitrifying organisms present.

111

2. Materials and methods

2.1. Reactor set-up and operation

Two previously acquired thermophilic nitrifying sequencing batch reactors (SBR) were transformed to membrane bioreactors (MBR) and are further mentioned as '$MBR_{T,constant}$' (Courtens et al., 2016a) and '$MBR_{T,increase}$' (Courtens et al., 2016b), referring to the applied development strategy, being the 'constant temperature enrichment' and 'temperature increase' strategy respectively as mentioned in the introduction. Submerged hollow fiber microfiltration membrane units, with a pore size of 100 nm, were constructed for *in situ* effluent extraction. The fibers originated from a full scale PALL Microza installation (Asahi Kasei Chemicals Corporation, Japan). Level controllers (Velleman, Belgium) were used to regulate the reactor volume around 2L. The reactor vessels were jacketed and controlled at a temperature of 50°C by use of circulating thermostatic water baths (Julabo MA-4). Overhead stirrers provided mixing and aquarium pumps were connected to diffuser stones for aeration. Dissolved oxygen concentration (DO) was controlled at 2 mg O_2 L^{-1} (Liquiline M CM442). The pH was controlled between 7.2 and 7.5 by dosing 0.2 M NaOH/HCl. Both reactors were continuously fed with synthetic medium consisting of $(NH_4)_2SO_4$ (150 mg N L^{-1}), 12 g $NaHCO_3$ g^{-1} N, KH_2PO_4 (10 mg P L^{-1}) and 0.1 mL L^{-1} trace elements (Kuai and Verstraete, 1998). To change the nitrogen loading rate, the flow rate was adjusted. $MBR_{T,constant}$ was characterized by robust and stable operation, despite several technical issues yielding short-term lower performance (**Figure S.5**). In $MBR_{T,increase}$, after transforming from SBR to MBR, the temperature was successfully increased from 48.5 to 50°C (**Figure S.6**). Based on the nitrogen balance, nitrogen loss through ammonia stripping or biomass assimilation was limited to 8 ± 12 and 7 ± 10% of total influent nitrogen in $MBR_{T,constant}$ and $MBR_{T,increase}$ respectively, indicating that nitrification was the main process of ammonia removal. Experiments with both reactors were only conducted during stable volumetric operation as

indicated in **Figure S.5 and S.6**. The two reactors were mainly operated for redundancy. As, to the author's knowledge, these were the only thermophilic nitrifying bioreactors in the world, a technical issue resulting in reactor failure would endanger the research on thermophilic nitrogen removal. Having two reactors at hand allows for more certainty of active biomass for other experiments outside this study. It was, thus, not the main goal to see differences between both reactors, even though both had a different development strategy.

2.2. Biokinetics

2.2.1. Biomass yield, maximum specific activity and maximum growth rate

The maximum biomass yield of the thermophilic AOA and NOB ($Y_{max,AOA}$ and $Y_{max,NOB}$) were determined based on stable isotope incorporation during activity measurements, as previously described (Vandekerckhove et al., 2019). The maximum biomass-specific ammonium (q_{max,NH_4^+-N}) and nitrite oxidation rates (q_{max,NO_2^--N}) were derived during these incubations as well. Taking into account the relative abundance of AOA and NOB at the time of the experiment, the group-specific rates of AOA ($q_{max,AOA}$) and NOB ($q_{max,NOB}$) could be derived. Moreover, the maximum AOA and NOB growth rate ($\mu_{max,AOA}$ and $\mu_{max,NOB}$) was calculated as the product of Y_{max} and q_{max}. Propagation of uncertainty was used to derive the 95% confidence interval.

2.2.3. Decay rate

To determine the decay rate (k_d), 400 mL of sludge was transferred to a temperature controlled respirometry setup. Continuous aeration was applied in the absence of substrate. On a daily basis, aeration was stopped to determine the endogenous oxygen uptake rate (OUR_{end}). Subsequently, the maximum oxygen uptake rate (OUR_{max}) in the presence of 5 mg NO_2^--N L^{-1} was obtained. After subtracting the OUR_{end}, a measure of the NOB activity was acquired. Finally, as a measure of the AOA activity, the NOB activity was subtracted from

the OUR_{max} (considering OUR_{end}) after dosing 5 mg NH_4^+-N L^{-1}. These measurements lasted between 0.2 and 0.7 hours. The decreasing $OUR_{max,AOA}$ and $OUR_{max,NOB}$ with time was exponential and equation 1 was fitted to the data.

$$OUR_{max,t} = OUR_{max,t0} * e^{-k_d * t} \quad (1)$$

With $OUR_{max,t}$ and $OUR_{max,t0}$ the maximum oxygen uptake rate at time point t and at the beginning of the experiment (t0) respectively. The k_d was estimated in Python, using the pyIDEAS package (Van Daele et al., 2015), using the Nelder-Mead algorithm for parameter optimization. To estimate the 95% confidence intervals, the inverse of the Fisher Information Matrix was calculated to obtain a linear approximation of the covariance matrix (Omlin and Reichert, 1999).

2.2.4. Apparent substrate affinity index

For both communities, the apparent affinity index for ammonium ($K_{s,N,AOA}$), nitrite ($K_{s,N,NOB}$) and oxygen ($K_{s,O,AOA}$ and $K_{s,O,NOB}$) was determined using *ex situ* respirometric measurements. Details can be found in Supplementary material, section S.2. The particle size distribution (PSD) was determined using the video channel of an EyeTech particle size analyzer (Ankersmid, Netherlands), as it can influence the apparent affinity index through diffusion limitation.

2.3. Susceptibility towards environmental factors

The susceptibility of the AOA and NOB of both thermophilic communities towards pH, temperature, salt, ammonium, free ammonia (NH_3/FA), nitrite and free nitrous acid (HNO_2/FNA) was determined using *ex situ* batch activity measurements in 96 Well plates with a working volume of 250 µL, similar as previously described (Courtens et al., 2016a). Plates were incubated at 50°C and shaken at 600 rpm in a Thermoshaker (Hangzhou Allsheng Instruments, Hangzhou, China). The buffer solution contained a final concentration of 0.3-0.6

185 g P L^{-1} (KH_2PO_4/K_2HPO_4), 0.5 g $NaHCO_3$ L^{-1}, 0.2 g $MgSO_4x7H_2O$ L^{-1}, 0.1 g $CaCL_2$, 0.1 mL
186 L^{-1} trace elements and $(NH_4)_2SO_4$ or $NaNO_2$.

187 Operational parameters such as pH, temperature and substrate concentration varied
188 depending on the investigated parameter. All three parameters were measured in the tests to
189 enable the calculation of FA and FNA concentrations using their chemical equilibrium
190 (Anthonisen et al., 1976). A combination of different tests uncoupled the effect of different
191 parameters (**Table S.1 and S.2**). All treatments were performed in quadruple or sextuple.
192 Liquid samples (2 µL) were taken over time for NH_4^+ and NO_2^- analysis. Biomass
193 concentration was determined using the concentration in the homogenized inoculum sample
194 (executed in triplicate) and the imposed dilution in the well plate.

195 **2.4. Molecular analysis**

196 Samples for full-length 16S rRNA gene SMRT amplicon sequencing were taken on day 1403
197 and 729 of operation in the $MBR_{T,constant}$ and $MBR_{T,increase}$ respectively. Samples for 16S
198 rRNA gene amplicon sequencing were taken at the time of the stable isotope experiment
199 (2.2.1.), being day of operation 1905 and 1230 in the $MBR_{T,constant}$ and $MBR_{T,increase}$
200 respectively. Samples were taken and stored at -20°C prior to DNA extraction. In parallel
201 with 16S rRNA gene amplicon sequencing, total bacteria and archaea were quantitatively
202 determined by qPCR. More information on the DNA extraction, amplicon sequencing and
203 data processing and qPCR analysis can be found in Supplementary material, section S.3 and
204 S.4.

205 The qPCR results and the biomass concentration of the samples were combined to yield total
206 bacteria and archaea in copies g^{-1} VSS. Together, they quantitatively represented the total
207 community. When considering the relative abundance of ammonia oxidizing bacteria (AOB)
208 and nitrite oxidizing bacteria (NOB) in the bacterial community and ammonia oxidizing

archaea (AOA) in the archaeal community, as determined by 16S rRNA gene amplicon sequencing, an estimation was made of the relative abundance of each microbial group. Recent research combining flow cytometry and sequencing has proven the significance of combining absolute and relative abundances and proposed the tandem qPCR and sequencing as valuable alternative to flow cytometry (Props et al., 2017).

2.5. Chemical analyses

Details on methods applied to determine ammonium, nitrite, nitrate, biomass concentration and bulk ^{13}C abundance can be found in Supplementary material, section S.5.

2.6. Statistical analyses

Statistical analysis was applied to check for significant differences in the obtained yield. Details can be found in Supplementary material, section S.6.

3. Results & discussion

3.1. Microbial community

A phylogenetic tree was constructed for the AOA, containing the abundance-based representative full 16S rRNA gene sequences of all OTUs present in $MBR_{T,constant}$ and $MBR_{T,increase}$ with more than one read over both reactors and 410 sequences from the *Nitrososphaera* and *Nitrosopumilales* (according to EMBL-taxonomy in SILVA release 132, **Figure 1**). The most abundant OTU (OTU 1, comprising 89.87% and 77.24% of the archaeal community in $MBR_{T,constant}$ and $MBR_{T,increase}$ respectively) was related to the *Nitrososphaera* genus, but clustered relatively far from the closest known species *Nitrososphaera gargensis* (on average 95.5% identity in the trimmed alignment). This might hint at the presence of a new species. However, genome-resolved shotgun metagenomics is required to attribute the necessary (functional) genes to this OTU to validate that it is responsible for the observed ammonia oxidation. Nonetheless, given the high abundance and the classification within the *Nitrososphaera* genus, known to oxidize ammonia, it is likely that this OTU is responsible for the conversion and, thus, represents a novel *Nitrososphaera* species. The closest uncultured relative (100% sequence identity in the trimmed alignment space) was a *Nitrososphaera* species (JX047156), found in a marine hot spring (58.5-68.5°C) from Kalianda Island, Indonesia (Xu et al., 2013).

The phylogenetic tree for NOB contained abundance-based representative sequences of all OTUs classified as either in the phylum Chloroflexi or the phylum Nitrospira and 105 reference sequences of the phyla Chloroflexi and Nitrospira (**Figure 2**). The two most abundant OTUs were classified as *Nitrospira* spp. and were closely related to *Nitrospira calida* (97% identity as opposed to 87.3% identity to the next closest related cultivated *Nitrospira*, *Nitrospira defluvii*).

On day 1905 and 1230 of operation in $MBR_{T,constant}$ and $MBR_{T,increase}$, amplicon sequencing and qPCR were used to estimate the absolute and relative abundance of AOA and NOB. The absolute (and relative) abundance of bacteria and archaea in $MBR_{T,constant}$, determined by qPCR, was found to be $3.1x10^{13} \pm 7.9x10^{12}$ copies (43 ± 16%) and $4.1x10^{13} \pm 1.0x10^{13}$ copies 57 ± 21%) respectively. In $MBR_{T,increase}$, this was $2.1x10^{13} \pm 6.3x10^{12}$ copies (24 ± 16%) and $6.4x10^{13} \pm 3.7x10^{13}$ copies (76 ± 49%) respectively. In both cultures, no AOB were found based on 16S rRNA amplicon sequencing. The bacterial community consisted of 26% and 22% *Nitrospira*-related NOB $MBR_{T,constant}$ and $MBR_{T,increase}$ respectively. The archaeal community in $MBR_{T,constant}$ comprised of 95% *Nitrososphaera*-related and 5% *Nitrosocosmicus*-related AOA, whereas in $MBR_{T,increase}$ 100% of the archaeal community was related to *Nitrososphaera*. applying the bacterial and archaeal community composition on the qPCR-based relative abundance of bacteria and archaea rendered an AOA relative abundance of 56.8 ± 17.9% and 75.5 ± 55.0% and a NOB relative abundance of 11.2 ± 4.1% and 5.4 ± 3.5% in $MBR_{T,constant}$ and $MBR_{T,increase}$ respectively. These communities were highly enriched in AOA, whereas less enriched in NOB compared to previous studies on thermophilic nitrification in a bioreactor (Courtens et al., 2016a, Courtens et al., 2016b).

3.2. Thermophilic biomass yield

To the authors best knowledge, only one study reported an observed yield of 0.067 g VSS g^{-1} N at 48°C (Courtens et al., 2016b). The observed yield (Y_{obs}) takes into account both growth and decay/maintenance, whereas the maximum yield only includes growth instantly obtained from oxidizing ammonia or nitrite (Metcalf et al., 2003). A new method was developed, based on ^{13}C incorporation (Vandekerckhove et al., 2019). It enables a fast determination of the maximum yield of a specific group of organisms in a mixed culture and renders the work-intensive isolation or enrichment unnecessary. No significant difference in $Y_{max,AOA}$ and $Y_{max,NOB}$ was observed when comparing both communities ($p>0.05$), with AOA values of

0.16 ± 0.01 and 0.20 ± 0.02 g VSS g^{-1} N and NOB values of 0.040 ± 0.005 and 0.043 ± 0.002 g VSS g^{-1} N for $MBR_{T,constant}$ and $MBR_{T,increase}$ respectively. The maximum AOA yield was remarkably higher than a reported mesophilic AOA yield of 0.09 g dry mass g^{-1} N (Könneke et al., 2014). Furthermore, lower mesophilic AOB yields (0.06-0.11 g VSS g^{-1} N) were obtained using the same method based on ^{13}C incorporation (Vandekerckhove et al., 2019), linked to a more efficient pathway for CO_2 incorporation of AOA compared to AOB (Könneke et al., 2014). Compared to other AOB yields in literature, the thermophilic AOA yield is within the range of 0.03-0.3 g VSS g^{-1} N (**Table S.5**). The thermophilic *Nitrospira* yield was in the same range of its mesophilic counterpart (0.048-0.051 g VSS g^{-1} N) when determined based on ^{13}C incorporation. It was, however, higher than the thermophilic *Nitrospira* yield determined previously (0.025-0.028 g VSS g^{-1} N) by the same method (Vandekerckhove et al., 2019). It is also in the same range of other reported mesophilic yields for *Nitrospira* (0.049-0.15 g VSS g^{-1} N) or *Nitrobacter* (0.040-072 g VSS g^{-1} N) (**Table S.6**). The discrepancy between the AOA and NOB yield in the studied mixed cultures is reflected in the community enrichment, as AOA were far more abundant than NOB. The overall nitrification yield was 0.20-0.24 g VSS g^{-1} N, which is in the same order of magnitude as previously determined (0.24-0.25 g VSS g^{-1} N) and exceeded the mesophilic yield (0.16 and 0.10 g VSS g^{-1} N at 15 and 28°C respectively), determined using ^{13}C incorporation (Vandekerckhove et al., 2019).

3.3. Growth kinetics

The q_{max,NH_4^+-N} amounted up to 517 ± 43 and 455 ± 30 mg N g^{-1} VSS_{tot} d^{-1} and a q_{max,NO_2^--N} of 358 ± 6 and 417 ± 20 mg N g^{-1} VSS_{tot} d^{-1} was obtained for $MBR_{T,constant}$ and $MBR_{T,increase}$ respectively. Taking into account the relative abundance of AOA (56.8% and 75.5%) and NOB (11.2% and 5.4%), AOA-specific rates of 0.91 ± 0.30 and 0.61 ± 0.44 g N g^{-1} VSS d^{-1}

and NOB-specific rates of 3.2 ± 1.0 and 7.7 ± 4.2 g N g^{-1} VSS d^{-1} were estimated for $MBR_{T,constant}$ and $MBR_{T,increase}$ respectively. The $q_{max,AOA}$ were low compared to reported literature values (0.67-6.85 g N g^{-1} VSS d^{-1}), whereas the $q_{max,NOB}$ were similar to mesophilic *Nitrospira* (3.3-8.9 g N g^{-1} VSS d^{-1}) and low compared to *Nitrobacter* (9.6-72 g N g^{-1} VSS d^{-1}) (**Table S.4 and S.6**).

Multiplying q_{max} and Y_{max} yielded estimated μ_{max} values of 0.15 ± 0.05 and 0.12 ± 0.09 d^{-1} for *Nitrososphaera* and 0.13 ± 0.05 and 0.33 ± 0.22 d^{-1} for *Nitrospira* in $MBR_{T,constant}$ and $MBR_{T,increase}$ respectively. The $\mu_{max,AOA}$ was similar to the growth rate of *Candidatus Nitrosocaldus islandicus* of 0.128 d^{-1} (Daebeler et al., 2017), but lower than other described AOA (0.32-0.8 d^{-1}) (**Table S.4**). The thermophilic *Nitrospira* growth rate was lower than literature values for mesophilic *Nitrospira* (0.38-0.52 d^{-1}) and *Nitrobacter* (0.23-2.6 d^{-1}) (**Table S.6**). Until this study, the decay rate for thermophilic AOA and NOB has not been determined yet. The $k_{d,AOA}$ in $MBR_{T,constant}$ and $MBR_{T,increase}$ was 0.231 ± 0.002 and 0.285 ± 0.002 d^{-1} respectively and the $k_{d,NOB}$ was 0.315 ± 0.002 and 0.429 ± 0.003 d^{-1} respectively (**Figure S.8**). These values were within the range reported in literature of mesophilic AOB (0.03-0.43 d^{-1}) and NOB (0.03-1.7 d^{-1}) (**Table S.5 and S.6**). As sludge proliferated in the bioreactors, k_d could not be higher than μ_{max}. A rough calculation based on a VSS and N balance in the MBR reactors demonstrated biomass growth (Y_{obs}: 0.028-0.035 g VSS g^{-1} N) at very high SRT (88-182 days), yielding estimated decay rates between 0.026-0.078 d^{-1}. This indicates that the experimentally determined k_d values were overestimated. It is known that k_d can vary depending on the conditions in a reactor system and comprises maintenance energy, real decay of cells, protozoa grazing,… (Salem et al., 2006). It is possible that the transfer from continuous feeding in the reactors to prolonged (17 days) stressful starvation induced a faster decay or that the inactivation rate was determined rather than the actual decay rate. The decay rate from batch experiments was measured indirectly via the oxygen uptake rate in the

presence of substrate instead of directly using biomass concentration measurements. A potential lag phase in maximum activity was not taken into account. A clear distinction was noticeable between endogenous respiration, nitrite oxidation and ammonia oxidation, so there was active oxidation measured (**Figure S.9**). Whether actual death of micro-organisms occurred or if a transitions to starvation conditions with lower metabolic activity took place, remains uncertain. Biochemical adjustments in a cell under starvation are called the stringent response process, in which energy is redirected to maintenance and overall activity is slowed down, resulting in a lower oxygen uptake rate (Mason et al., 1986). In addition to the overestimated k_d, an underestimation of μ_{max} was possible as well. The loading rate in the MBR reactors was only 28 ± 6 and 35 ± 12% of q_{max,NH_4^+-N} in $MBR_{T,constant}$ and $MBR_{T,increase}$ respectively, meaning growth conditions were not optimal and *in situ* growth rates (μ) were smaller than μ_{max}. As biomass growth was observed in the MBRs, μ is bound to be higher than k_d and, thus, so must μ_{max} be. The obtained values for μ_{max} were possibly underestimated by the fact that VSS includes other particulate matter in addition to biomass (Metcalf et al., 2003). Molecular tools as qPCR and Illumina sequencing might have introduced a bias as well. In literature, the simultaneous determination of nitrifier μ_{max} and k_d mostly involved model fitting to steady-state reactor data, batch test data or respirometry assays as opposed to experimental determination as performed in this study (Ahn et al., 2008, Hanaki et al., 1990, Kappeler and Brodmann, 1995, Munz et al., 2008, Nowak et al., 1995, Park and Noguera, 2007). Despite the possible underestimation of μmax, it might be that the obtained thermophiles were slow growing. Issues of experimentally determined k_d values being higher than μ_{max} were not reported for faster growing aerobic heterotrophs converting organic carbon, but it was shown that *in situ* versus batch-wise determination of μ_{max} and k_d yielded different results, with an overestimation of k_d in batch experiments. It was suggested to use

the *in situ* estimated decay and the intrinsic μ_{max} as obtained batch-wise (Vogelaar et al., 2003).

3.4. Apparent substrate affinity index

Substrate affinity plays an important role in niche differentiation and in the attainable effluent nitrogen concentration in wastewater treatment facilities. The apparent affinity index of AOA for ammonium and oxygen in both reactors were similar, with $K_{S,N,AOA}$ of 0.36 ± 0.04 and 0.32 ± 0.02 mg N L^{-1} and $K_{S,O,AOA}$ of 0.13 ± 0.09 and 0.21 ± 0.15 mg O_2 L^{-1} for $MBR_{T,constant}$ and $MBR_{T,increase}$ respectively (**Figure 3, A and B and Figure 4, A and B**). The obtained apparent AOA affinity indices for ammonium were remarkably higher than previously reported for AOA (0.002-0.030 mg N L^{-1}) and for comammox (**Table S.7**). The thriving reactor conditions in this study, as opposed to planktonic conditions in AOA enrichment studies, elicits the influence of advectional and diffusional factors, such as floc size, oxygen/substrate gradient, mixing intensity, reactor hydraulics,… on the apparent affinity indices (Arnaldos et al., 2015). Although mixing was intensive, floc size was relatively small (D90 = 33.24-35.28 µm) (**Figure S.7**) and biomass concentration was not unusually high in this study, it cannot be excluded that these factors had an influence. It has even been shown that microcolonies (<16 µm) within flocs affect the apparent affinity index (Picioreanu et al., 2016). The biomass concentration during these experiments was higher in $MBR_{T,increase}$ (4.45-4.85 g VSS L^{-1}) than in $MBR_{T,constant}$ (2.95-3.85 g VSS L^{-1}), meaning that more diffusional and advectional resistance might have occurred. To properly reflect actual conditions in practical applications, the determination of substrate affinity under the influence of these physical resistances in bioreactors is essential. The obtained apparent affinity indices are thus more likely to prevail in real-life applications rather than the indices derived from single-cell cultures. Compared to AOB affinities (0.07-46.2 mg N L^{-1}), determined in bioreactors, these apparent affinity indices are quite low (**Table S.7**). Low $K_{s,N,AOA}$ is in accordance with

368 literature, as AOA are often found in oligotrophic environments (Erguder et al., 2009). The
369 $K_{s,O,AOA}$ (0.13-0.21 mg O_2 L^{-1}) was in the range of previously reported values (0.06-0.33 mg
370 O_2 L^{-1}) (**Table S.7**). Considering possible advectional and diffusional resistances in this study
371 compared to literature, the actual affinity index could be higher. Compared to AOB (0.18-
372 5.95 mg O_2 L^{-1}) (**Table S.7**), the obtained apparent affinity index is low, indicative of
373 literature statements on AOA niche differentiation and presence in oxygen-limited habitats
374 (Erguder et al., 2009).

375 The NOB in $MBR_{T,increase}$ had a slightly lower apparent affinity index for nitrite and oxygen
376 (0.27 ± 0.05 mg N L^{-1} and 0.15 ± 0.05 mg O_2 L^{-1}) than the NOB of $MBR_{T,constant}$ (1.23 ± 0.3
377 mg N L^{-1} and 0.55 ± 0.27 mg O_2 L^{-1}) (**Figure 3, C and D and Figure 4, C and D**). The
378 $K_{s,N,NOB}$ and $K_{s,O,NOB}$ values were within the range of reported affinity indices of mesophilic
379 *Nitrospira* (0.11-0.9 mg N L^{-1} and 0.13-0.54 mg O_2 L^{-1}) and *Nitrobacter* (0.009-9.59 mg N L^{-1}
380 and 0.25-1.66 mg O_2 L^{-1}) apparent affinity indices (**Table S.8**).

381 **3.5. Robustness of thermophilic nitrification**

382 When developing biotechnological solutions for nitrogen in wastewater, it is important to
383 acknowledge that abiotic factors are not stable. Practical application requires a robust
384 community that can deal with stress situations. However, a properly controlled system
385 prevents the occurrence of conditions to which the process is sensitive, meaning the
386 sensitivity of a microbial process should not hinder its application. As nitrification can be
387 regarded as the most vulnerable process in common nitrification/denitrification or
388 nitritation/denitritation, this study evaluated the capacity of the thermophilic cultures to deal
389 with differences in substrate concentration, pH, temperature and salts. To properly assess the
390 susceptibility, it must also be tested in long-term experiments, as opposed to the short-term
391 batch experiments performed in this study.

With regard to substrate inhibition, it is important to distinguish between the chemical forms in equilibrium, being ammonium/ammonia and nitrite/free nitrous acid. Fluctuations in temperature, pH and substrate concentration in wastewater treatment facilities affect the substrate speciation and, thus, the possible inhibition of nitrification. The AOA in both reactors were not susceptible to ammonium and FA concentrations up to 300 and 16 mg N L^{-1} (**Figure 5, A**), which is in accordance with two previous studies on AOA (Courtens et al., 2016a, Sauder et al., 2017). However, they were more tolerant than other AOA enrichments, reporting full inhibition in the range of 14-280 mg NH_4^+-N L^{-1} and 0.252-10.5 mg NH_3-N L^{-1} (Hatzenpichler, 2012). Substrate accumulation might have a different effect on various species, as substrate concentration has been hypothesized to drive niche differentiation within *Thaumarchaeota* (Sauder et al., 2017). The concentrations in a bioreactor can be considered higher than most oligotrophic environments from which AOA have been isolated and characterized, thus selecting for more tolerant species. In addition, although biomass flocs were small in this study, diffusional and advectional resistance might have been higher compared to cellular batch enrichments of the previous studies. This resistance could yield lower substrate concentrations on a planktonic level, thus rendering the organisms more tolerant to higher bulk concentrations. Furthermore, both thermophilic communities were highly tolerant to salts, with an IC_{50} for AOA of about 40 g NaCl L^{-1} of added salinity (92.3 mS cm^{-1}) and for NOB of about 20 g NaCl L^{-1} of added salinity (50.5 mS cm^{-1}). The limited effect of salt on nitrification activity expands the application possibilities to salty nitrogenous streams (**Figure S.10**). Temperatures down to 40°C retained more than 70% of the nitrification activity (**Figure 6**). Biomass from $MBR_{T,increase}$, which was originally derived from mesophilic nitrifying sludge (Courtens et al., 2016b), could cope best with lower temperatures, retaining 100% AOA and more than 85% NOB activity. As problems with nitrification often arise when temperatures exceed 40°C (Henze, 1997), these findings are

promising and suggest that the presence of the correct nitrifying species can expand the boundaries of current practices and enable nitrogen removal at a broad temperature range. Increasing temperatures, on the other hand, have proven to be detrimental to nitrite oxidation from 55°C and to ammonia oxidation from 60°C onwards.

3.6. Opportunities for short-cut nitrogen removal

In case nitratation could be prevented via smart process control, short-cut nitrogen removal could be established via nitritation/denitritation or partial nitrification/anammox, rendering economic and ecological benefits (Peng et al., 2017, Vlaeminck et al., 2012). Besides NOB suppression, thermophilic anammox should be established as well. Recently, anammox activity was reported for 2 weeks at 50°C in an up-flow anaerobic sludge blanket reactor (UASB) (Zhang et al., 2018).

Several strategies for NOB suppression have been proposed (Agrawal et al., 2018, Vlaeminck et al., 2012). They involve FA or FNA shock therapy (NOB are more susceptible to FA/FNA (Anthonisen et al., 1976)), working at decreased oxygen concentrations (AOB have a lower apparent oxygen affinity index than NOB (Blackburne et al., 2008)) and decreasing the SRT to wash out NOB while retaining AOB (due to lower growth rate of NOB at sidestream conditions (Hellinga et al., 1998)).

The tolerance of nitrite oxidation towards FA and NH_4^+ in this study (IC_{50} > 16 mg NH_3-N L^{-1} and 250 mg NH_4^+-N L^{-1}) (**Figure 5, B**) was much higher than the reported range of 0.1-1 mg NH_3-N L^{-1} (Anthonisen et al., 1976) and the previously described IC_{50} of 5 mg NH_3-N L^{-1} (Courtens et al., 2016a). The use of a FA shock-therapy to suppress nitratation will, thus, be challenging at thermophilic temperatures. The communities in this study were clearly inhibited by nitrite, whereas free nitrous acid is usually depicted as inhibiting rather than nitrite (**Figure 5, B and D**). FNA acts as a protonophore, which increases proton

441 permeability through cell membranes. This counteracts the proton pumping effect of ATPase,
442 thus inhibiting ATP synthesis. Furthermore, FNA may force bacteria to turn on- or off
443 particular enzymes to defend against its toxicity, may affect gene transcriptional processes
444 and mislead the enzyme assemblage and may directly react with enzymes involved in the
445 metabolic processes (Zhou et al., 2011). The inhibitory effect of nitrite to the thermophilic
446 AOA and NOB remains to be investigated. Especially the NOB were highly susceptible to
447 nitrite, with an IC_{50} of 40 mg NO_2^--N L^{-1} compared to 1.5-2 g NO_2^--N L^{-1} for AOA, opening
448 up opportunities if nitrite accumulation can be established. As NOB in the studied bioreactor
449 communities were more resilient to changing pH than AOA (**Figure 6, C and D**), changing
450 the pH to mediate nitrite accumulation is difficult. The optimum pH for AOA of both reactors
451 was 6.9, retaining more than 60% of the activity in the range of 6.5-7.9 (**Figure 6, A**). The
452 NOB proved to withstand pH changes better, with an optimum of 6.7 in both reactors and
453 over 80% and 90% remaining activity in the range of 6.4-7.8 for $MBR_{T,constant}$ and
454 $MBR_{T,increase}$ respectively (**Figure 6, C**). Increasing the temperature, on the other hand, could
455 facilitate the inhibition of nitratation, as the NOB activity was severely declined at 55°C
456 whereas the AOA activity remained unaffected (**Figure 6, A and B**). The NOB apparent
457 oxygen affinity index in $MBR_{T,increase}$ was similar to the AOA apparent oxygen affinity (0.21
458 ± 0.15 and 0.15 ± 0.05 mg O_2 L^{-1} respectively), whereas in $MBR_{T,constant}$ the AOA displayed a
459 lower apparent oxygen affinity index compared to NOB affinity (0.13 ± 0.09 and 0.55 ± 0.27
460 mg O_2 L^{-1} respectively). Mediating NOB out-selection by aeration control would, thus, only
461 be possible in $MBR_{T,constant}$. This renders the need for kinetic characterization of every
462 nitrifying community before qualifying for aeration control to enable short-cut nitrogen
463 removal. Finally, the strategy of aggressive SRT control does not seem feasible at
464 thermophilic temperatures, as the NOB maximum growth rate (0.13-0.33 d^{-1}) was higher

when compared to AOA (0.12-0.15 d^{-1}). Overall, this study shows that current strategies for NOB suppression might prove difficult at thermophilic temperatures.

4. Conclusions

This study characterized the stoichiometry and kinetics of two thermophilic nitrifying bioreactor communities. The most abundant archaeal OTU was related to the *Nitrososphaera* genus, but clustered relatively far from the known species *Nitrososphaera gargensis* (95.5% identity). The most abundant NOB were related to *Nitrospira calida* (97% identity). Thermophilic nitrification yield was 0.20-0.24 g VSS g^{-1} N, resulting mainly from a high AOA yield (0.16-0.20 g VSS g^{-1} N), which was reflected in a higher AOA abundance (57-76%) compared to NOB (5-11%). Batch-wise determination of decay rates (AOA: 0.23-0.29 d^{-1}; NOB: 0.32-0.43 d^{-1}) rendered overestimated values compared to *in situ* estimation of the total decay rate (0.026-0.078 d^{-1}), possibly because the inactivation rate was determined in the batch experiments rather than the actual decay rate. Estimations of maximum growth rates (AOA: 0.12-0.15 d^{-1}; NOB: 0.13-0.33 d^{-1}) were low and possibly underestimated. Apparent substrate affinity indices were low, as is indicative of thermophilic nitrifying organisms. A high NOB susceptibility towards nitrite accumulation (IC_{50}: 40 mgNO_2^--N L^{-1}) is favorable for developing shortcut nitrogen removal. However, NOB had a high growth rate and low apparent oxygen affinity index (0.15-0.55 mg O_2 L^{-1}) and were resilience towards free ammonia (IC_{50} >16mg NH_3-N L^{-1}). This might complicate NOB outselection using common practices (SRT control; aeration control; free ammonia shocks). Overall, the obtained insights in thermophilic nitrification can assist in integrating thermophilic conversions to facilitate single-sludge nitrification/denitrification and possibly nitritation/denitritation.

Acknowledgements

The authors acknowledge (i) the Agency for Innovation by Science and Technology (IWT Flanders) [grant number SB-141205] for funding Tom G.L. Vandekerckhove, (ii) Waterboard De Dommel for funding Chaïm De Mulder, (iii) Geconcerteerde Onderzoeksactie (GOA) from Ghent University (BOF17/GOA/032 and BOF15/GOA/006) for funding Frederiek-Maarten, (iv) Samuel Bodé for performing the ^{13}C analysis, (v) Sophie Balemans for the help with the processing of the particle size distribution data, (vi) Tim Lacoere for helping in DNA extraction and processing of the 16S rRNA gene amplicon sequencing data and (vii) Bart De Gusseme from Farys/UGent for providing the hollow fiber membranes.

References

Agrawal, S., Seuntjens, D., De Cocker, P., Lackner, S. and Vlaeminck, S.E. (2018) Success of mainstream partial nitritation/anammox demands integration of engineering, microbiome and modeling insights. Current Opinion in Biotechnology 50, 214-221.

Ahn, J.H., Yu, R. and Chandran, K. (2008) Distinctive microbial ecology and biokinetics of autotrophic ammonia and nitrite oxidation in a partial nitrification Bioreactor. Biotechnology and Bioengineering 100(6), 1078-1087.

Anthonisen, A.C., Loehr, R.C., Prakasam, T.B.S. and Srinath, E.G. (1976) Inhibition of Nitrification by Ammonia and Nitrous-Acid. Journal Water Pollution Control Federation 48(5), 835-852.

Arnaldos, M., Amerlinck, Y., Rehman, U., Maere, T., Van Hoey, S., Naessens, W. and Nopens, I. (2015) From the affinity constant to the half-saturation index: Understanding conventional modeling concepts in novel wastewater treatment processes. Water Research 70, 458-470.

Baker, B.J., Lesniewski, R.A. and Dick, G.J. (2012) Genome-enabled transcriptomics reveals archaeal populations that drive nitrification in a deep-sea hydrothermal plume. Isme Journal 6(12), 2269-2279.

Blackburne, R., Yuan, Z.G. and Keller, J. (2008) Partial nitrification to nitrite using low dissolved oxygen concentration as the main selection factor. Biodegradation 19(2), 303-312.

Camargo, J.A. and Alonso, A. (2006) Ecological and toxicological effects of inorganic nitrogen pollution in aquatic ecosystems: A global assessment. Environment International 32(6), 831-849.

Coppens, J., Meers, E., Boon, N., Buysse, J. and Vlaeminck, S.E. (2016) Follow the N and P road: High-resolution nutrient flow analysis of the Flanders region as precursor for sustainable resource management. Resources Conservation and Recycling 115, 9-21.

Courtens, E.N.P., Boon, N., De Schryver, P. and Vlaeminck, S.E. (2014a) Increased salinity improves the thermotolerance of mesophilic nitrification. Applied Microbiology and Biotechnology 98(10), 4691-4699.

Courtens, E.N.P., Spieck, E., Vilchez-Vargas, R., Bode, S., Boeckx, P., Schouten, S., Jauregui, R., Pieper, D.H., Vlaeminck, S.E. and Boon, N. (2016a) A robust nitrifying community in a bioreactor at 50°C opens up the path for thermophilic nitrogen removal. Isme Journal 10(9), 2293-2303.

Courtens, E.N.P., Vandekerckhove, T., Prat, D., Vilchez-Vargas, R., Vital, M., Pieper, D.H., Meerbergen, K., Lievens, B., Boon, N. and Vlaeminck, S.E. (2016b) Empowering a mesophilic inoculum for thermophilic nitrification: Growth mode and temperature pattern as critical proliferation factors for archaeal ammonia oxidizers. Water Research 92, 94-103.

Courtens, E.N.P., Vlaeminck, S.E., Vilchez-Vargas, R., Verliefde, A., Jauregui, R., Pieper, D.H. and Boon, N. (2014b) Trade-off between mesophilic and thermophilic denitrification: Rates vs. sludge production, settleability and stability. Water Research 63, 234-244.

Daebeler, A., Herbold, C., Vierheilig, J., Sedlacek, C.J., Pjevac, P., Albersten, M., Kirkegaard, R.H., de la Torre, J.R., Daims, H. and Wagner, M. (2017) Cultivation and genomic analysis of Candidatus Nitrosocaldus islandicus, a novel obligately thermophilic ammonia-oxidizing Thaumarchaeon. bioRxiv.

de la Torre, J.R., Walker, C.B., Ingalls, A.E., Konneke, M. and Stahl, D.A. (2008) Cultivation of a thermophilic ammonia oxidizing archaeon synthesizing crenarchaeol. Environmental Microbiology 10(3), 810-818.

Dodsworth, J.A., Hungate, B.A. and Hedlund, B.P. (2011) Ammonia oxidation, denitrification and dissimilatory nitrate reduction to ammonium in two US Great Basin hot springs with abundant ammonia-oxidizing archaea. Environmental Microbiology 13(8), 2371-2386.

Edwards, T.A., Calica, N.A., Huang, D.A., Manoharan, N., Hou, W.G., Huang, L.Q., Panosyan, H., Dong, H.L. and Hedlund, B.P. (2013) Cultivation and characterization of thermophilic Nitrospira species from geothermal springs in the US Great Basin, China, and Armenia. Fems Microbiology Ecology 85(2), 283-292.

Erguder, T.H., Boon, N., Wittebolle, L., Marzorati, M. and Verstraete, W. (2009) Environmental factors shaping the ecological niches of ammonia-oxidizing archaea. Fems Microbiology Reviews 33(5), 855-869.

Hanaki, K., Wantawin, C. and Ohgaki, S. (1990) Nitrification at Low-Levels of Dissolved-Oxygen with and without Organic Loading in a Suspended-Growth Reactor. Water Research 24(3), 297-302.

570
571 Hatzenpichler, R. (2012) Diversity, Physiology, and Niche Differentiation of Ammonia-Oxidizing
572 Archaea. Applied and Environmental Microbiology 78(21), 7501-7510.
573
574 Hatzenpichler, R., Lebedeva, E.V., Spieck, E., Stoecker, K., Richter, A., Daims, H. and Wagner, M.
575 (2008) A moderately thermophilic ammonia-oxidizing crenarchaeote from a hot spring. Proceedings
576 of the National Academy of Sciences of the United States of America 105(6), 2134-2139.
577
578 Hellinga, C., Schellen, A.A.J.C., Mulder, J.W., van Loosdrecht, M.C.M. and Heijnen, J.J. (1998) The
579 SHARON process: An innovative method for nitrogen removal from ammonium-rich waste water.
580 Water Science and Technology 37(9), 135-142.
581
582 Henze, M. (1997) Wastewater Treatment: Biological and Chemical Processes, Springer.
583
584 Henze, M., Gujer, W., Mino, T. and van Loosdrecht, M.C.M. (2000) Activated sludge models ASM1,
585 ASM2, ASM2d and ASM3, IWA Publishing.
586
587 Henze, M., van Loosdrecht, M.C.M., Ekama, G.A. and Brdjanovic, D. (2008) Biological wastewater
588 treatment, IWA Publishing.
589
590 Kappeler, J. and Brodmann, R. (1995) Low F/M Bulking and Scumming - Towards a Better
591 Understanding by Modeling. Water Science and Technology 31(2), 225-234.
592
593 Könneke, M., Schubert, D.M., Brown, P.C., Hügler, M., Standfest, S., Schwander, T., Schada von
594 Borzyskowski, L., Erb, T.J., Stahl, D.A. and Berg, I.A. (2014) Ammonia-oxidizing archaea use the most
595 energy-efficient aerobic pathway for CO₂ fixation. Proceedings of the National
596 Academy of Sciences 111(22), 8239-8244.
597
598 Kuai, L.P. and Verstraete, W. (1998) Ammonium removal by the oxygen-limited autotrophic
599 nitrification-denitrification system. Applied and Environmental Microbiology 64(11), 4500-4506.
600
601 Lapara, T.M. and Alleman, J.E. (1999) Thermophilic aerobic biological wastewater treatment. Water
602 Research 33(4), 895-908.
603
604 Lebedeva, E.V., Alawi, M., Fiencke, C., Namsaraev, B., Bock, E. and Spieck, E. (2005) Moderately
605 thermophilic nitrifying bacteria from a hot spring of the Baikal rift zone. Fems Microbiology Ecology
606 54(2), 297-306.
607
608 Lebedeva, E.V., Hatzenpichler, R., Pelletier, E., Schuster, N., Hauzmayer, S., Bulaev, A., Grigor'eva,
609 N.V., Galushko, A., Schmid, M., Palatinszky, M., Le Paslier, D., Daims, H. and Wagner, M. (2013)
610 Enrichment and Genome Sequence of the Group I. 1a Ammonia-Oxidizing Archaeon "Ca.
611 Nitrosotenuis uzonensis" Representing a Clade Globally Distributed in Thermal Habitats. Plos One
612 8(11).
613

614 Lebedeva, E.V., Off, S., Zumbragel, S., Kruse, M., Shagzhina, A., Lucker, S., Maixner, F., Lipski, A.,
615 Daims, H. and Spieck, E. (2011) Isolation and characterization of a moderately thermophilic nitrite-
616 oxidizing bacterium from a geothermal spring. Fems Microbiology Ecology 75(2), 195-204.

617
618 Marks, C.R., Stevenson, B.S., Rudd, S. and Lawson, P.A. (2012) Nitrospira-dominated biofilm within a
619 thermal artesian spring: a case for nitrification-driven primary production in a geothermal setting.
620 Geobiology 10(5), 457-466.

621
622 Martens-Habbena, W., Berube, P.M., Urakawa, H., de la Torre, J.R. and Stahl, D.A. (2009) Ammonia
623 oxidation kinetics determine niche separation of nitrifying Archaea and Bacteria. Nature 461(7266),
624 976-U234.

625
626 Metcalf, amp and Eddy, I. (2003) Wastewater engineering : treatment and reuse, Fourth edition /
627 revised by George Tchobanoglous, Franklin L. Burton, H. David Stensel. Boston : McGraw-Hill, [2003]
628 ©2003.

629
630 Munz, G., Gori, R., Cammilli, L. and Lubello, C. (2008) Characterization of tannery wastewater and
631 biomass in a membrane bioreactor using respirometric analysis. Bioresource Technology 99(18),
632 8612-8618.

633
634 Nowak, O., Svardal, K. and Schweighofer, P. (1995) The dynamic behaviour of nitrifying activated
635 sludge systems influenced by inhibiting wastewater compounds. Water Science and Technology
636 31(2), 115-124.

637
638 Omlin, M. and Reichert, P. (1999) A comparison of techniques for the estimation of model prediction
639 uncertainty. Ecological Modelling 115(1), 45-59.

640
641 Park, H.D. and Noguera, D.R. (2007) Characterization of two ammonia-oxidizing bacteria isolated
642 from reactors operated with low dissolved oxygen concentrations. Journal of Applied Microbiology
643 102(5), 1401-1417.

644
645 Peng, L., Carvajal-Arroyo, J.M., Seuntjens, D., Prat, D., Colica, G., Pintucci, C. and Vlaeminck, S.E.
646 (2017) Smart operation of nitritation/denitritation virtually abolishes nitrous oxide emission during
647 treatment of co-digested pig slurry centrate. Water Research 127, 1-10.

648
649 Picioreanu, C., Perez, J. and van Loosdrecht, M.C.M. (2016) Impact of cell cluster size on apparent
650 half-saturation coefficients for oxygen in nitrifying sludge and biofilms. Water Research 106, 371-
651 382.

652
653 Props, R., Kerckhof, F.M., Rubbens, P., De Vrieze, J., Sanabria, E.H., Waegeman, W., Monsieurs, P.,
654 Hammes, F. and Boon, N. (2017) Absolute quantification of microbial taxon abundances. Isme
655 Journal 11(2), 584-587.

656
657 Reigstad, L.J., Richter, A., Daims, H., Urich, T., Schwark, L. and Schleper, C. (2008) Nitrification in
658 terrestrial hot springs of Iceland and Kamchatka. Fems Microbiology Ecology 64(2), 167-174.

Salem, S., Moussa, M.S. and van Loosdrecht, M.C.M. (2006) Determination of the decay rate of nitrifying bacteria. Biotechnology and Bioengineering 94(2), 252-262.

Sauder, L.A., Albertsen, M., Engel, K., Schwarz, J., Nielsen, P.H., Wagner, M. and Neufeld, J.D. (2017) Cultivation and characterization of Candidatus Nitrosocosmicus exaquare, an ammonia-oxidizing archaeon from a municipal wastewater treatment system. Isme Journal 11(5), 1142-1157.

Schouten, S., Hopmans, E.C. and Damste, J.S.S. (2013) The organic geochemistry of glycerol dialkyl glycerol tetraether lipids: A review. Organic Geochemistry 54, 19-61.

Shore, J.L., M'Coy, W.S., Gunsch, C.K. and Deshusses, M.A. (2012) Application of a moving bed biofilm reactor for tertiary ammonia treatment in high temperature industrial wastewater. Bioresource Technology 112, 51-60.

Sorokin, D.Y., Vejmelkova, D., Lucker, S., Streshinskaya, G.M., Rijpstra, W.I.C., Damste, J.S.S., Kleerbezem, R., van Loosdrecht, M., Muyzer, G. and Daims, H. (2014) Nitrolancea hollandica gen. nov., sp nov., a chemolithoautotrophic nitrite-oxidizing bacterium isolated from a bioreactor belonging to the phylum Chloroflexi. International Journal of Systematic and Evolutionary Microbiology 64, 1859-1865.

Spear, J.R., Barton, H.A., Robertson, C.E., Francis, C.A. and Pace, N.R. (2007) Microbial community biofabrics in a geothermal mine adit. Applied and Environmental Microbiology 73(19), 6172-6180.

Van Daele, T., Van Hoey, S. and Nopens, I. (2015) pyIDEAS: an Open Source Python Package for Model Analysis. 12th International Symposium on Process Systems Engineering (Pse) and 25th European Symposium on Computer Aided Process Engineering (Escape), Pt A 37, 569-574.

Vandekerckhove, T.G.L., Bodé, S., De Mulder, C., Vlaeminck, S.E. and Boon, N. (2019) 13C Incorporation as a Tool to Estimate Biomass Yields in Thermophilic and Mesophilic Nitrifying Communities. Frontiers in Microbiology 10(192).

Vlaeminck, S.E., De Clippeleir, H. and Verstraete, W. (2012) Microbial resource management of one-stage partial nitritation/anammox. Microbial Biotechnology 5(3), 433-448.

Vogelaar, J.C.T., Klapwijk, B., Temmink, H. and van Lier, J.B. (2003) Kinetic comparisons of mesophilic and thermophilic aerobic biomass. Journal of Industrial Microbiology & Biotechnology 30(2), 81-88.

Wang, S.F., Xiao, X., Jiang, L.J., Peng, X.T., Zhou, H.Y., Meng, J. and Wang, F.P. (2009) Diversity and Abundance of Ammonia-Oxidizing Archaea in Hydrothermal Vent Chimneys of the Juan de Fuca Ridge. Applied and Environmental Microbiology 75(12), 4216-4220.

Weidler, G.W., Gerbl, F.W. and Stan-Lotter, H. (2008) Crenarchaeota and their role in the nitrogen cycle in a subsurface radioactive thermal spring in the Austrian central Alps. Applied and Environmental Microbiology 74(19), 5934-5942.

Xu, S.-Y., He, P.-Q., Zilda, D.S., Zhang, X., Chasanah, E., Liu, T. and Huang, X.-H. (2013) Hydrogen-Producing Microflora and Fe–Fe Hydrogenase Diversities in Seaweed Bed Associated with Marine Hot Springs of Kalianda, Indonesia.

Zeng, G.M., Zhang, J.C., Chen, Y.N., Yu, Z., Yu, M., Li, H., Liu, Z.F., Chen, M., Lu, L.H. and Hu, C.X. (2011) Relative contributions of archaea and bacteria to microbial ammonia oxidation differ under different conditions during agricultural waste composting. Bioresource Technology 102(19), 9026-9032.

Zhang, Z.-Z., Ji, Y.-X., Cheng, Y.-F., Xu, L.-Z.-J. and Jin, R.-C. (2018) Increased salinity improves the thermotolerance of mesophilic anammox consortia. Science of The Total Environment 644, 710-716.

Zhou, Y., Oehmen, A., Lim, M., Vadivelu, V. and Ng, W.J. (2011) The role of nitrite and free nitrous acid (FNA) in wastewater treatment plants. Water Research 45(15), 4672-4682.

721 **Figure captions**

722 **Figure 1:** Phylogenetic relationships between abundance-based representative sequences of
723 all OTUs present in $MBR_{T,constant}$ and $MBR_{T,increase}$ with more than one read over both reactors
724 and 410 EMBL-classification sequences from the *Nitrososphaera* and *Nitrosopumilales*. The
725 OTU marked in blue was the most abundant AOA in the archaeal community of both
726 reactors.

727 **Figure 2:** Phylogenetic relationships between abundance-based representative sequences of
728 all OTUs present in $MBR_{T,constant}$ and $MBR_{T,increase}$ with more than one read over both reactors
729 and 146 reference sequences of the phyla *Chloroflexi* (SILVA release 132 LTP) and
730 *Nitrospira* (SILVA release 132 Ref with pintail quality assessed, 105 sequences). The OTUs
731 marked in blue were the most abundant NOB in the bacterial community of both reactors.

732 **Figure 3:** Determination of the affinity index for (A) ammonium of the AOA in $MBR_{T,constant}$,
733 (B) ammonium of AOA in $MBR_{T,increase}$, (C) nitrite of NOB in $MBR_{T,constant}$ and (D) nitrite of
734 the NOB in $MBR_{T,increase}$. Error bars represent the standard deviation on the online measured
735 oxygen uptake rate during each substrate spike (n=1), converted to the units mg N g^{-1} VSS d^{-1}
736 through error propagation.

737 **Figure 4:** Determination of the affinity index for oxygen of the (A) AOA in $MBR_{T,constant}$, (B)
738 AOA in $MBR_{T,increase}$, (C) NOB in $MBR_{T,constant}$ and (D) NOB in $MBR_{T,increase}$. Horizontal
739 error bars reflect the standard deviation on the average oxygen concentration during each
740 activity measurement. Vertical error bars represent the error on the linear slope fitted to the
741 declining substrate concentration during the activity measurements using the least squares
742 method. For each oxygen concentration, one activity measurement was performed.

743 **Figure 5:** The effect of ammonium/FA and nitrite/FNA concentrations on thermophilic
744 ammonium (A,C) and nitrite (B,D) oxidation. Each graph displays two complementary batch

activity measurements, at high (filled symbols) and low (empty symbols) FA/FNA levels, for the biomass from $MBR_{T,constant}$ (triangles) and $MBR_{T,increase}$ (circles). Full lines depict the remaining activity, whereas dotted lines represents the corresponding FA/FNA concentrations. Each data point signifies the average of quadruple activity measurements (technical replicates) and the error bars signify the error obtained through error propagation of the standard deviation of the volumetric activity and the biomass concentration.

Figure 6: The effect of pH and temperature on thermophilic ammonia (A,B) and nitrite (C,D) oxidation. Full lines depict the remaining activity for biomass from $MBR_{T,constant}$ (triangles) and $MBR_{T,increase}$ (circles), whereas the dotted line represents the corresponding FA/FNA concentrations. Each data point signifies the average of sextuple activity measurements (technical replicates) and the error bars signify the error obtained through error propagation of the standard deviation of the volumetric activity and the biomass concentration.

Figures

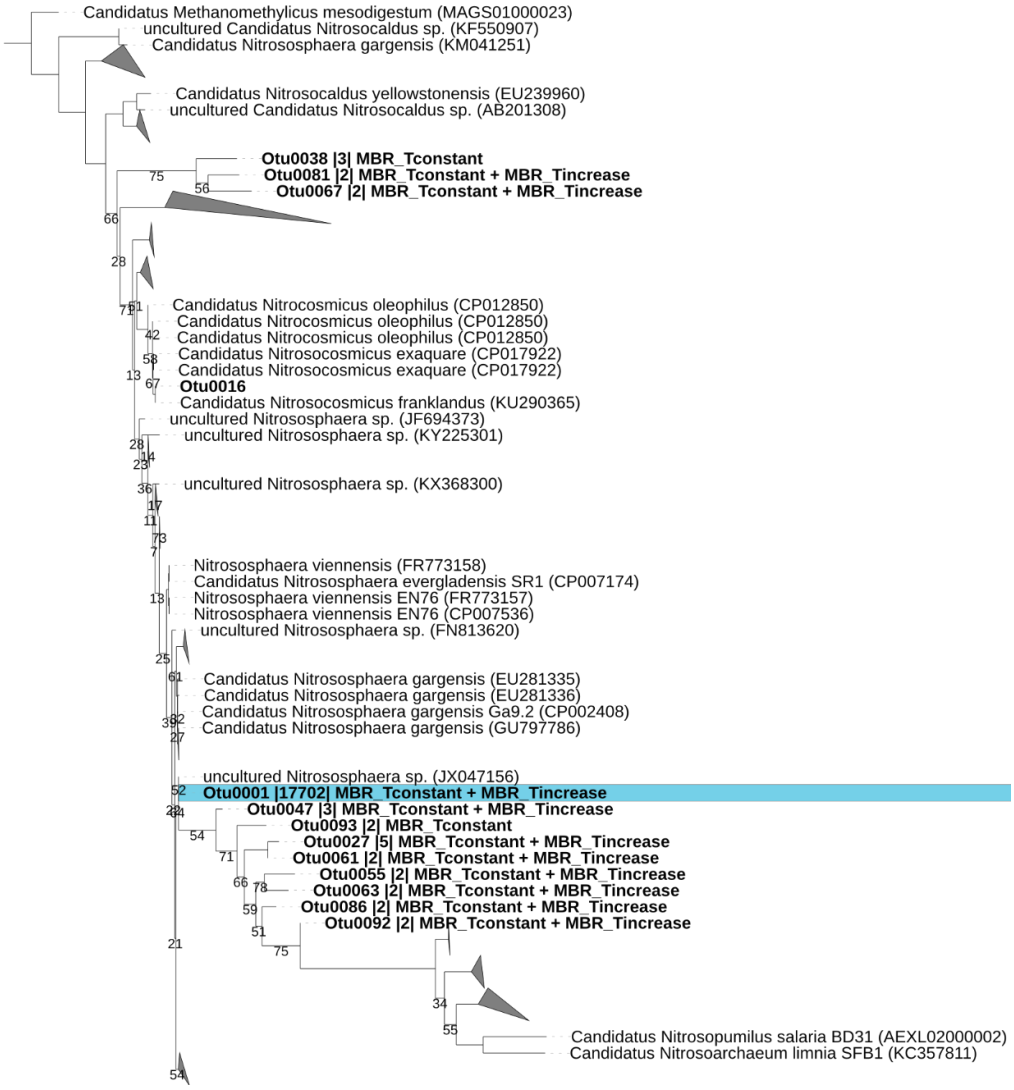
Tree scale: 0.1
Candidatus Methanomethylicus mesodigestum (MAGS01000023)
uncultured Candidatus Nitrosocaldus sp. (KF550907)
Candidatus Nitrososphaera gargensis (KM041251)
Candidatus Nitrosocaldus yellowstonensis (EU239960)
uncultured Candidatus Nitrosocaldus sp. (AB201308)
Otu0038 |3| MBR_Tconstant
Otu0081 |2| MBR_Tconstant + MBR_Tincrease
Otu0067 |2| MBR_Tconstant + MBR_Tincrease
Candidatus Nitrocosmicus oleophilus (CP012850)
Candidatus Nitrocosmicus oleophilus (CP012850)
Candidatus Nitrocosmicus oleophilus (CP012850)
Candidatus Nitrosocosmicus exaquare (CP017922)
Candidatus Nitrosocosmicus exaquare (CP017922)
Otu0016
Candidatus Nitrososocosmicus franklandus (KU290365)
uncultured Nitrososphaera sp. (JF694373)
uncultured Nitrososphaera sp. (KY225301)
uncultured Nitrososphaera sp. (KX368300)
Nitrososphaera viennensis (FR773158)
Candidatus Nitrososphaera evergladensis SR1 (CP007174)
Nitrososphaera viennensis EN76 (FR773157)
Nitrososphaera viennensis EN76 (CP007536)
uncultured Nitrososphaera sp. (FN813620)
Candidatus Nitrososphaera gargensis (EU281335)
Candidatus Nitrososphaera gargensis (EU281336)
Candidatus Nitrososphaera gargensis Ga9.2 (CP002408)
Candidatus Nitrososphaera gargensis (GU797786)
uncultured Nitrososphaera sp. (JX047156)
Otu0001 |17702| MBR_Tconstant + MBR_Tincrease
Otu0047 |3| MBR_Tconstant + MBR_Tincrease
Otu0093 |2| MBR_Tconstant
Otu0027 |5| MBR_Tconstant + MBR_Tincrease
Otu0061 |2| MBR_Tconstant + MBR_Tincrease
Otu0055 |2| MBR_Tconstant + MBR_Tincrease
Otu0063 |2| MBR_Tconstant + MBR_Tincrease
Otu0086 |2| MBR_Tconstant + MBR_Tincrease
Otu0092 |2| MBR_Tconstant + MBR_Tincrease
Candidatus Nitrosopumilus salaria BD31 (AEXL02000002)
Candidatus Nitrosoarchaeum limnia SFB1 (KC357811)

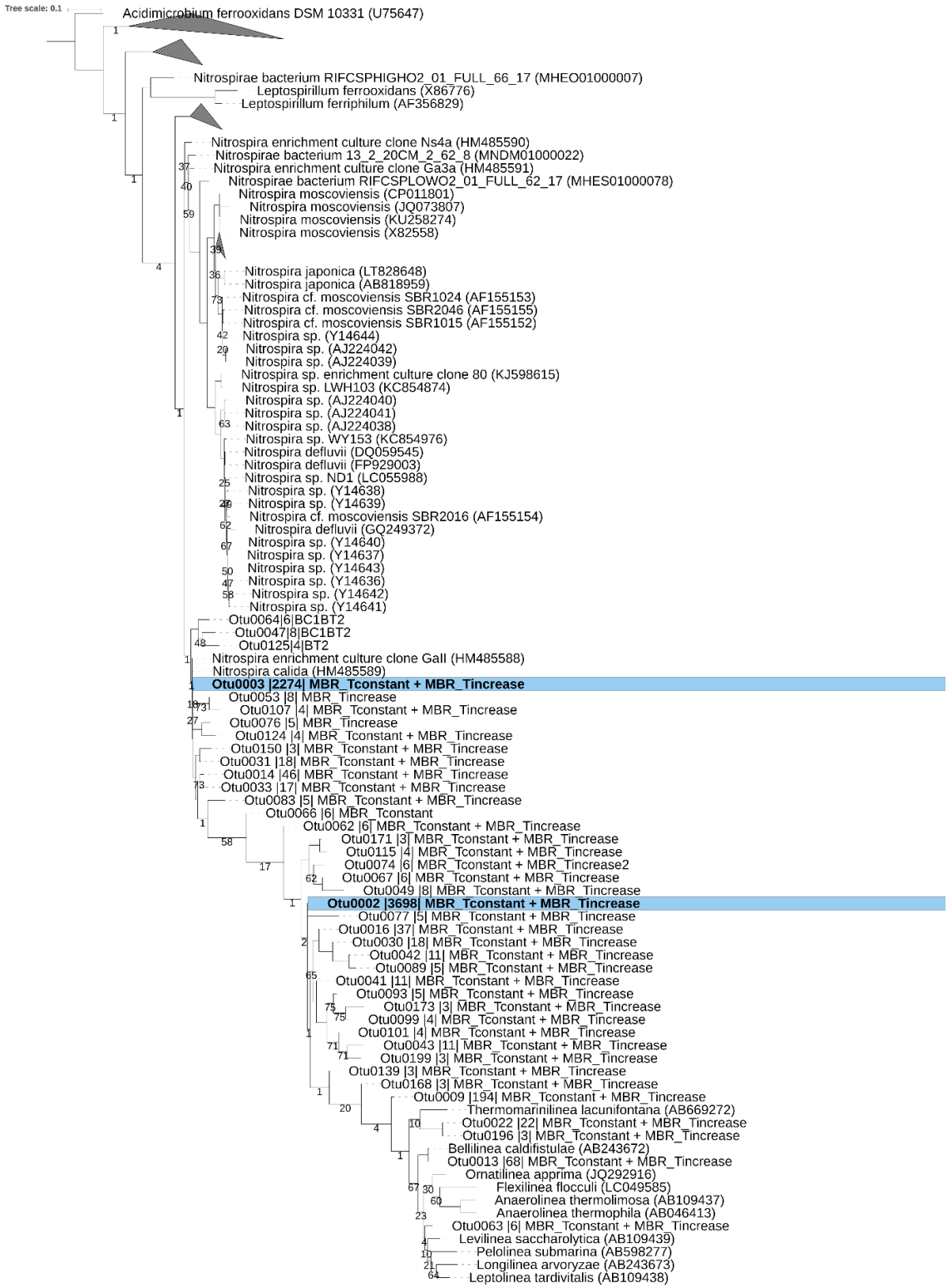
Tree scale: 0.1
Acidimicrobium ferrooxidans DSM 10331 (U75647)
Nitrospirae bacterium RIFCSPHIGHO2_01_FULL_66_17 (MHEO01000007)
Leptospirillum ferrooxidans (X86776)
Leptospirillum ferriphilum (AF356829)
Nitrospira enrichment culture clone Ns4a (HM485590)
Nitrospirae bacterium 13_2_20CM_2_62_8 (MNDM01000022)
Nitrospira enrichment culture clone Ga3a (HM485591)
Nitrospirae bacterium RIFCSPLOWO2_01_FULL_62_17 (MHES01000078)
Nitrospira moscoviensis (CP011801)
Nitrospira moscoviensis (JQ073807)
Nitrospira moscoviensis (KU258274)
Nitrospira moscoviensis (X82558)
Nitrospira japonica (LT828648)
Nitrospira japonica (AB818959)
Nitrospira cf. moscoviensis SBR1024 (AF155153)
Nitrospira cf. moscoviensis SBR2046 (AF155155)
Nitrospira cf. moscoviensis SBR1015 (AF155152)
Nitrospira sp. (Y14644)
Nitrospira sp. (AJ224042)
Nitrospira sp. (AJ224039)
Nitrospira sp. enrichment culture clone 80 (KJ598615)
Nitrospira sp. LWH103 (KC854874)
Nitrospira sp. (AJ224040)
Nitrospira sp. (AJ224041)
Nitrospira sp. (AJ224038)
Nitrospira sp. WY153 (KC854976)
Nitrospira defluvii (DQ059545)
Nitrospira defluvii (FP929003)
Nitrospira sp. ND1 (LC055988)
Nitrospira sp. (Y14638)
Nitrospira sp. (Y14639)
Nitrospira cf. moscoviensis SBR2016 (AF155154)
Nitrospira defluvii (GQ249372)
Nitrospira sp. (Y14640)
Nitrospira sp. (Y14637)
Nitrospira sp. (Y14643)
Nitrospira sp. (Y14636)
Nitrospira sp. (Y14642)
Nitrospira sp. (Y14641)
Otu0064|6|BC1BT2
Otu0047|8|BC1BT2
Otu0125|4|BT2
Nitrospira enrichment culture clone GaII (HM485588)
Nitrospira calida (HM485589)
Otu0003 |2274| MBR_Tconstant + MBR_Tincrease
Otu0053 |8| MBR_Tincrease
Otu0107 |4| MBR_Tconstant + MBR_Tincrease
Otu0076 |5| MBR_Tincrease
Otu0124 |4| MBR_Tconstant + MBR_Tincrease
Otu0150 |3| MBR_Tconstant + MBR_Tincrease
Otu0031 |18| MBR_Tconstant + MBR_Tincrease
Otu0014 |46| MBR_Tconstant + MBR_Tincrease
Otu0033 |17| MBR_Tconstant + MBR_Tincrease
Otu0083 |5| MBR_Tconstant + MBR_Tincrease
Otu0066 |6| MBR_Tconstant
Otu0062 |6| MBR_Tconstant + MBR_Tincrease
Otu0171 |3| MBR_Tconstant + MBR_Tincrease
Otu0115 |4| MBR_Tconstant + MBR_Tincrease
Otu0074 |6| MBR_Tconstant + MBR_Tincrease2
Otu0067 |6| MBR_Tconstant + MBR_Tincrease
Otu0049 |8| MBR_Tconstant + MBR_Tincrease
Otu0002 |3698| MBR_Tconstant + MBR_Tincrease
Otu0077 |5| MBR_Tconstant + MBR_Tincrease
Otu0016 |37| MBR_Tconstant + MBR_Tincrease
Otu0030 |18| MBR_Tconstant + MBR_Tincrease
Otu0042 |11| MBR_Tconstant + MBR_Tincrease
Otu0089 |5| MBR_Tconstant + MBR_Tincrease
Otu0041 |11| MBR_Tconstant + MBR_Tincrease
Otu0093 |5| MBR_Tconstant + MBR_Tincrease
Otu0173 |3| MBR_Tconstant + MBR_Tincrease
Otu0099 |4| MBR_Tconstant + MBR_Tincrease
Otu0101 |4| MBR_Tconstant + MBR_Tincrease
Otu0043 |11| MBR_Tconstant + MBR_Tincrease
Otu0199 |3| MBR_Tconstant + MBR_Tincrease
Otu0139 |3| MBR_Tconstant + MBR_Tincrease
Otu0168 |3| MBR_Tconstant + MBR_Tincrease
Otu0009 |194| MBR_Tconstant + MBR_Tincrease
Thermomarinilinea lacunifontana (AB669272)
Otu0022 |22| MBR_Tconstant + MBR_Tincrease
Otu0196 |3| MBR_Tconstant + MBR_Tincrease
Bellilinea caldifistulae (AB243672)
Otu0013 |68| MBR_Tconstant + MBR_Tincrease
Ornatilinea apprima (JQ292916)
Flexilinea flocculi (LC049585)
Anaerolinea thermolimosa (AB109437)
Anaerolinea thermophila (AB046413)
Otu0063 |6| MBR_Tconstant + MBR_Tincrease
Levilinea saccharolytica (AB109439)
Pelolinea submarina (AB598277)
Longilinea arvoryzae (AB243673)
Leptolinea tardivitalis (AB109438)

761

762

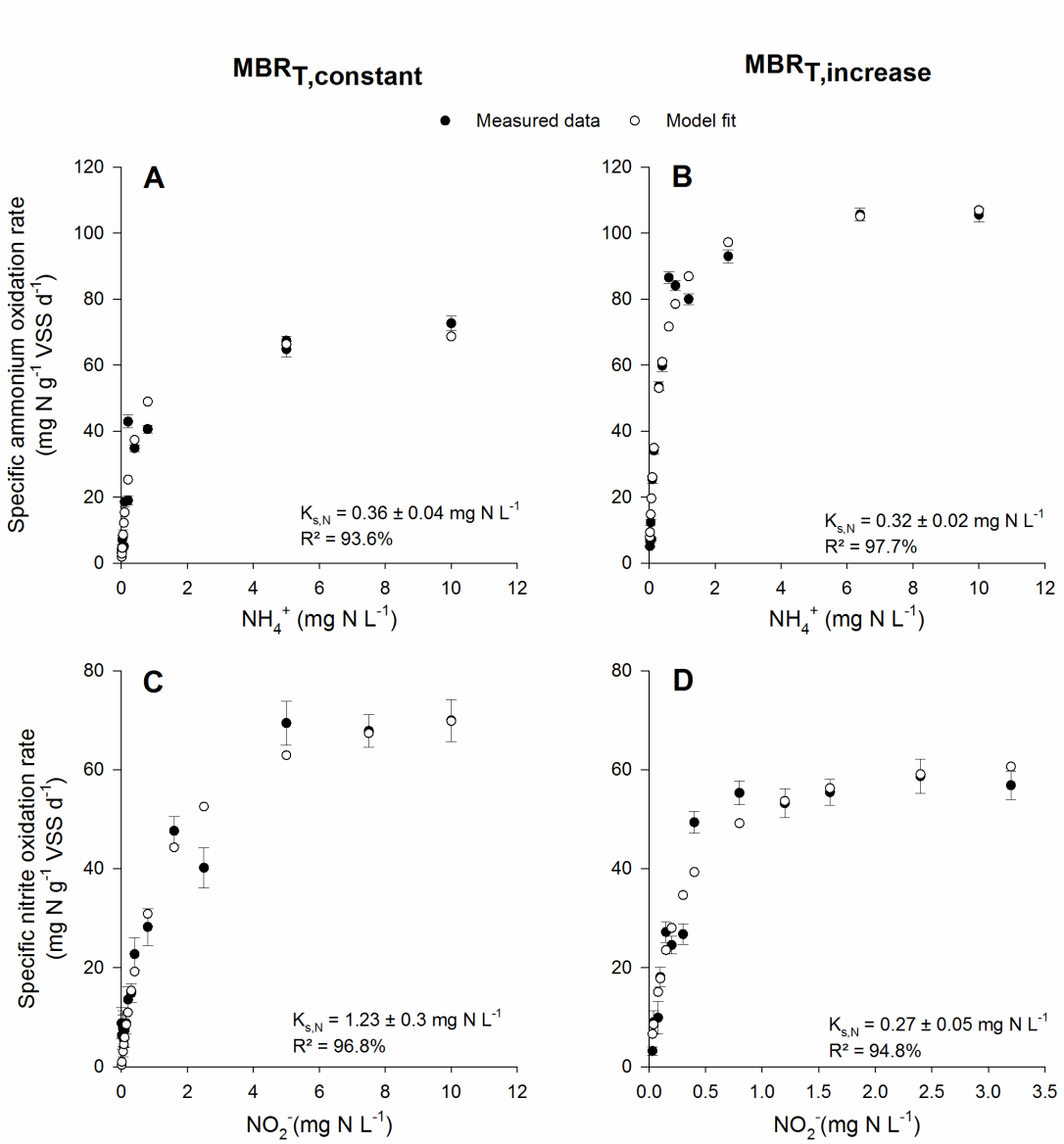
MBR T,constant
MBR T,increase
Measured data
Model fit
A
B
C
D
Specific ammonium oxidation rate (mg N g-1 VSS d-1)
Specific nitrite oxidation rate (mg N g-1 VSS d-1)
NH4+ (mg N L-1)
NO2-(mg N L-1)
Ks,N = 0.36 ± 0.04 mg N L-1
R² = 93.6%
Ks,N = 0.32 ± 0.02 mg N L-1
R² = 97.7%
Ks,N = 1.23 ± 0.3 mg N L-1
R² = 96.8%
Ks,N = 0.27 ± 0.05 mg N L-1
R² = 94.8%

763

764

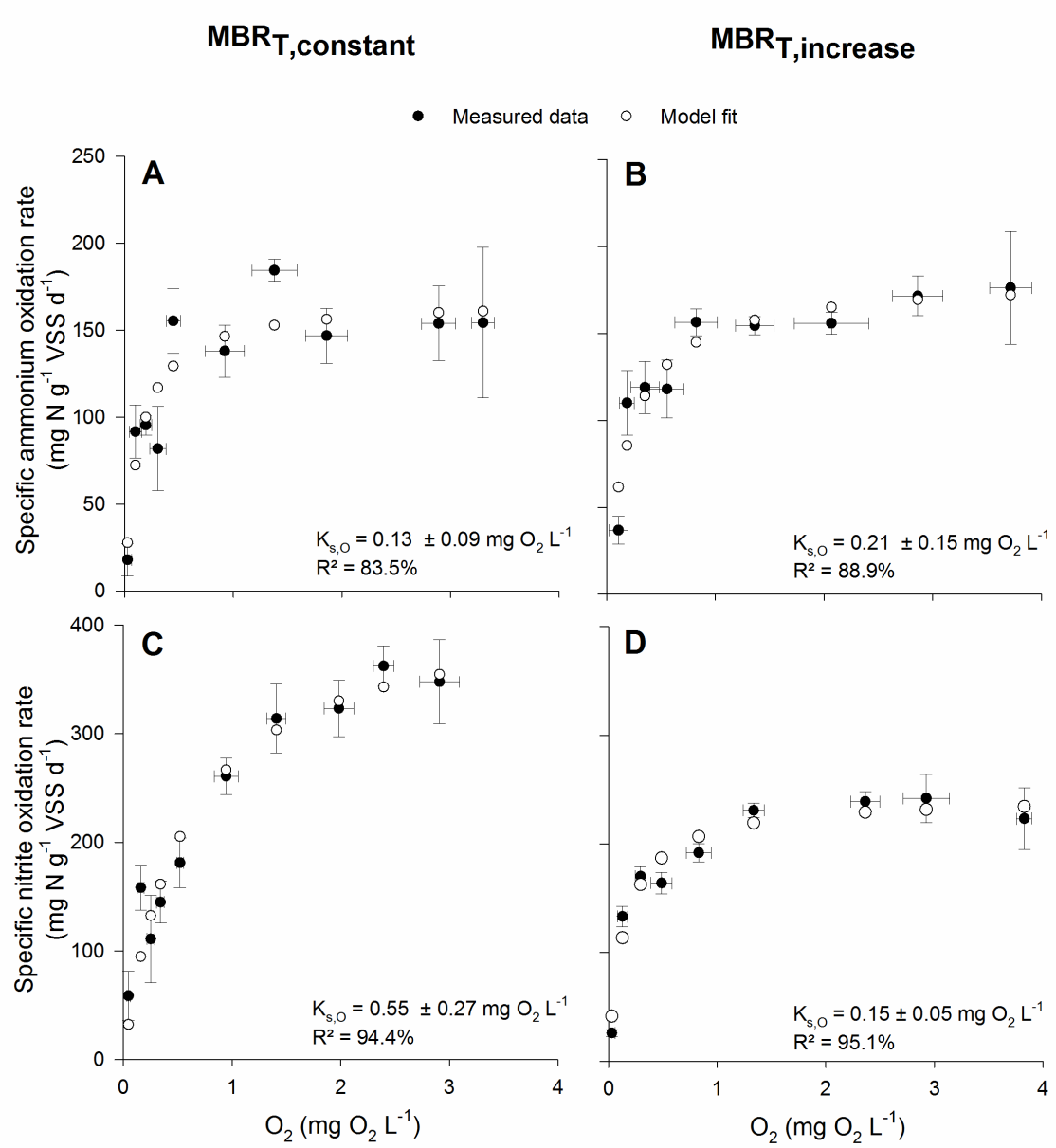
MBR T,constant
MBR T,increase
Measured data
Model fit
A
B
C
D
Specific ammonium oxidation rate (mg N g-1 VSS d-1)
Specific nitrite oxidation rate (mg N g-1 VSS d-1)
Ks,O = 0.13 ± 0.09 mg O2 L-1
R² = 83.5%
Ks,O = 0.21 ± 0.15 mg O2 L-1
R² = 88.9%
Ks,O = 0.55 ± 0.27 mg O2 L-1
R² = 94.4%
Ks,O = 0.15 ± 0.05 mg O2 L-1
R² = 95.1%
O2 (mg O2 L-1)
O2 (mg O2 L-1)

765

766

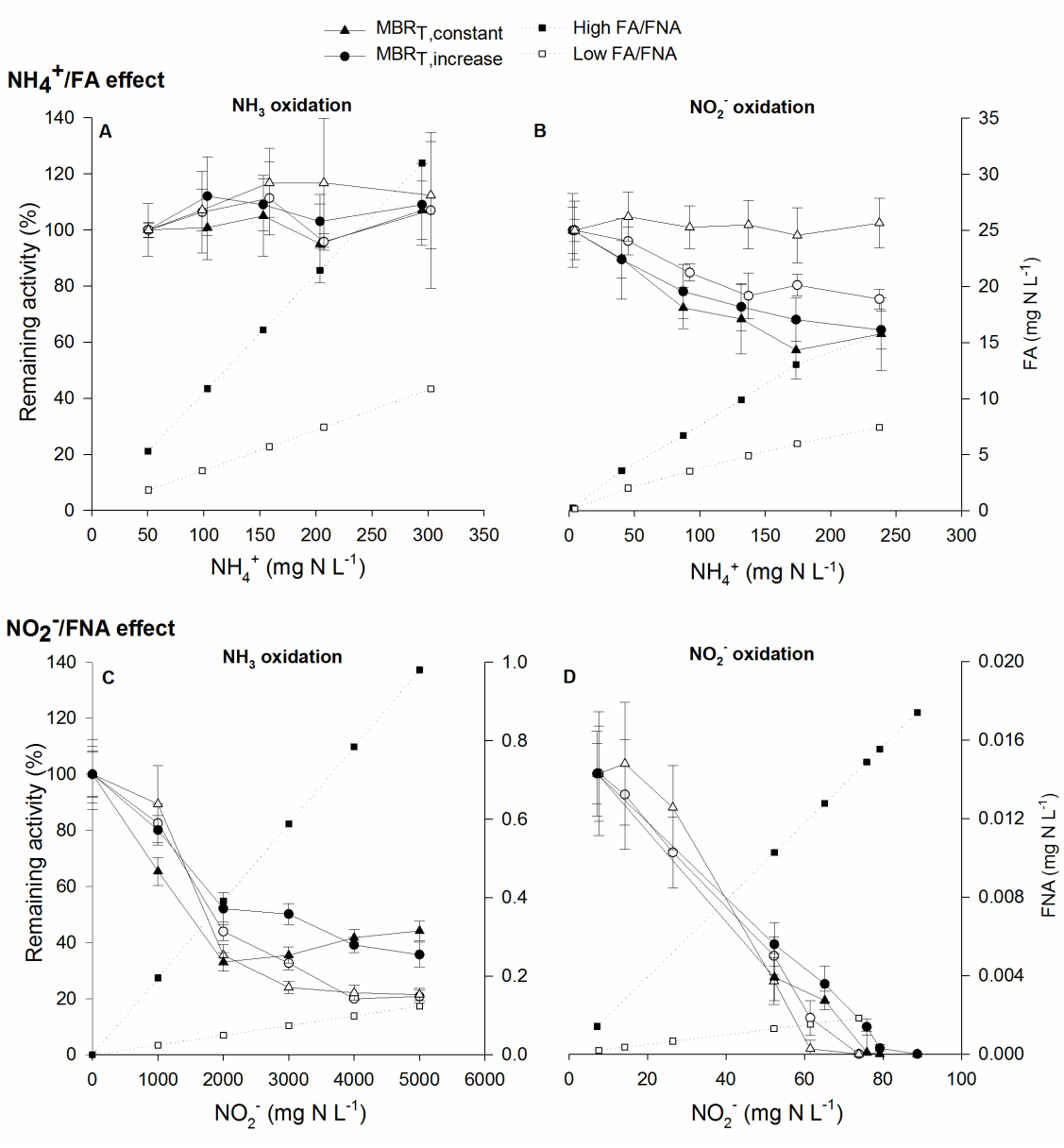
MBR$_{T,constant}$
MBR$_{T,increase}$
High FA/FNA
Low FA/FNA
NH$_4^+$/FA effect
NH$_3$ oxidation
A
Remaining activity (%)
NH$_4^+$ (mg N L^{-1})
NO$_2^-$ oxidation
B
FA (mg N L^{-1})
NH$_4^+$ (mg N L^{-1})
NO$_2^-$/FNA effect
NH$_3$ oxidation
C
Remaining activity (%)
NO$_2^-$ (mg N L^{-1})
NO$_2^-$ oxidation
D
FNA (mg N L^{-1})
NO$_2^-$ (mg N L^{-1})

767

768

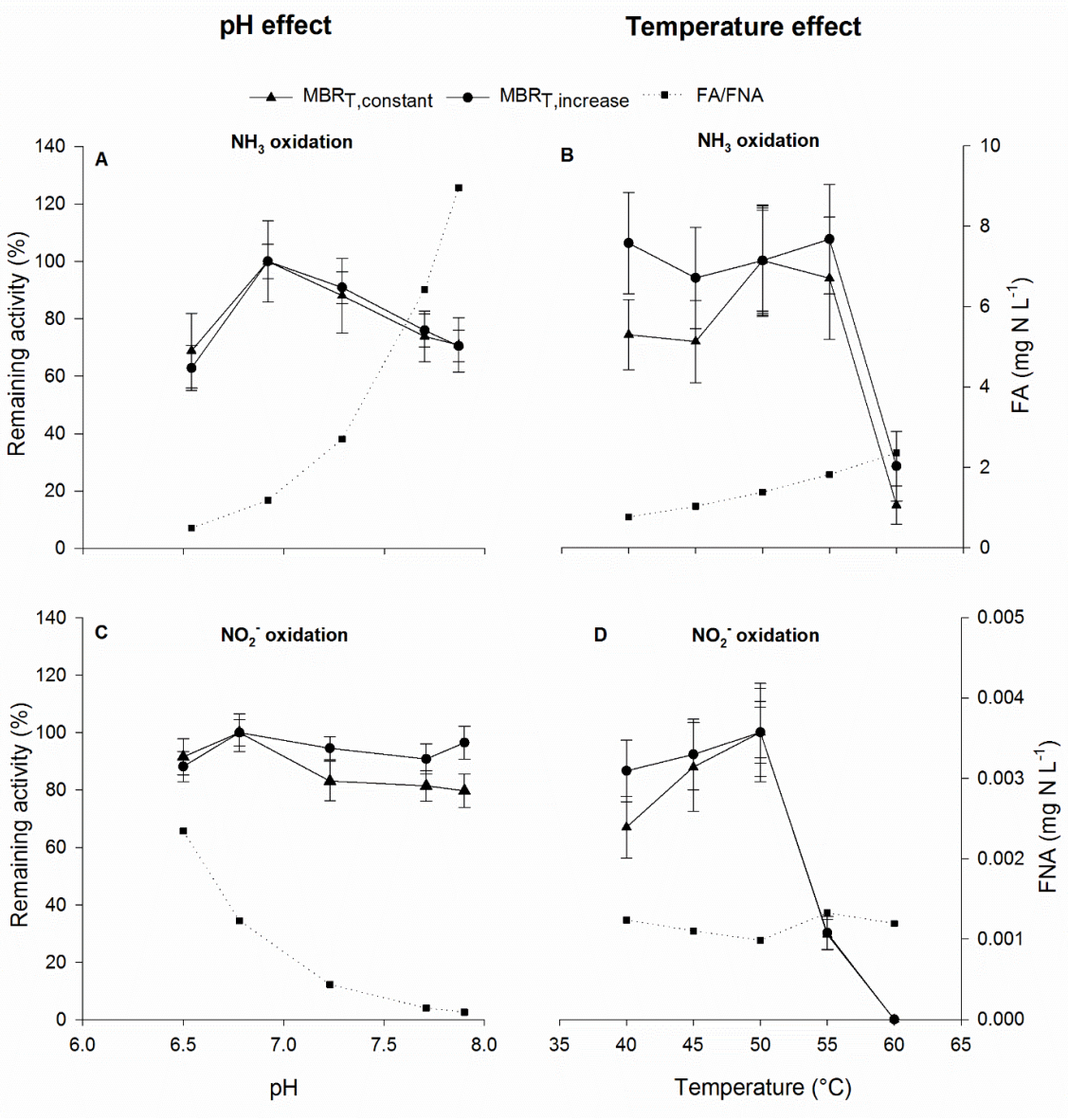
pH effect
Temperature effect
MBR$_{T,constant}$
MBR$_{T,increase}$
FA/FNA
A
B
C
D
NH$_3$ oxidation
NH$_3$ oxidation
NO$_2^-$ oxidation
NO$_2^-$ oxidation
Remaining activity (%)
Remaining activity (%)
FA (mg N L^{-1})
FNA (mg N L^{-1})
pH
Temperature (°C)

769

770

Figure 3
Click here to download high resolution image

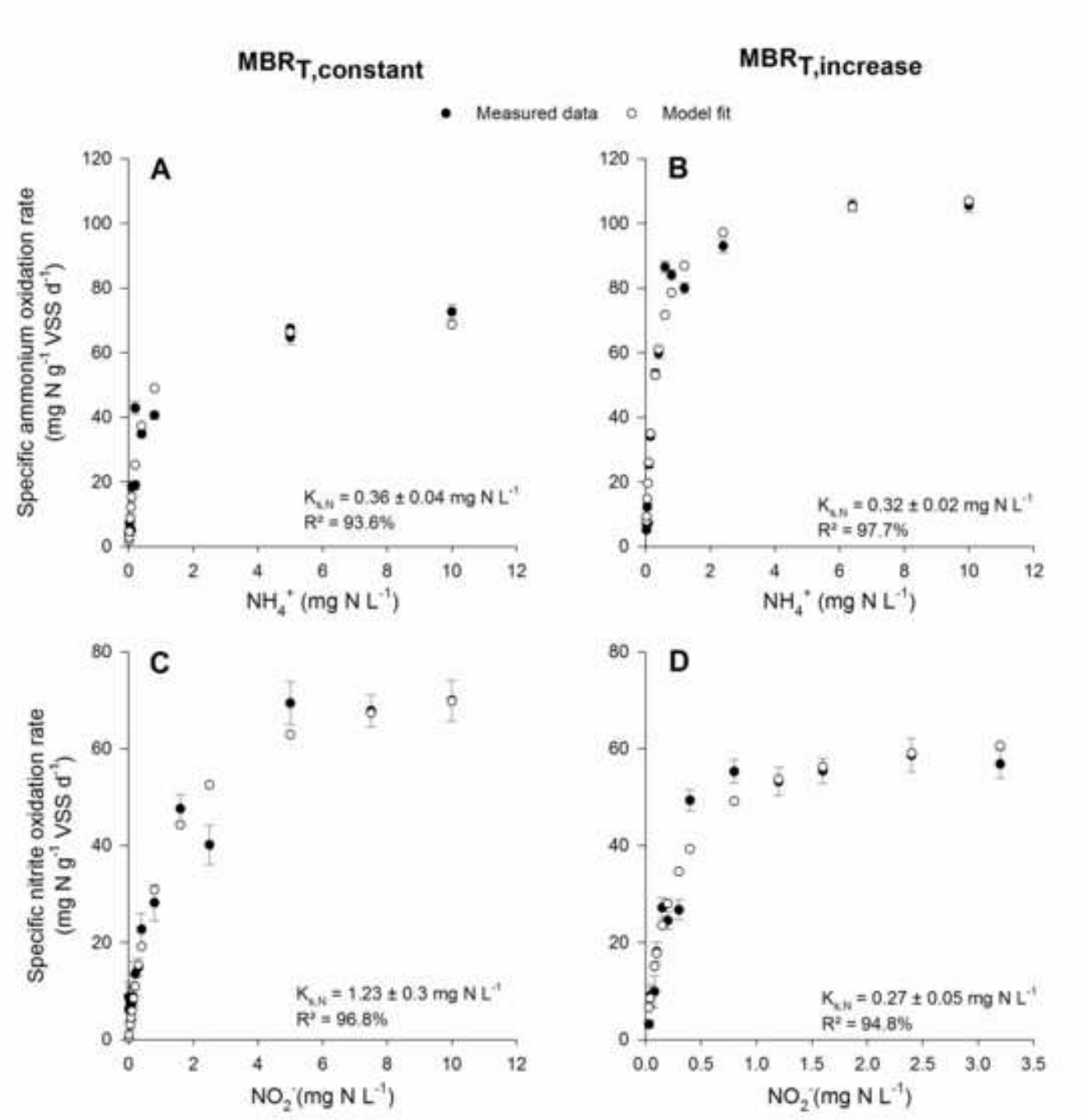

Figure 4
Click here to download high resolution image

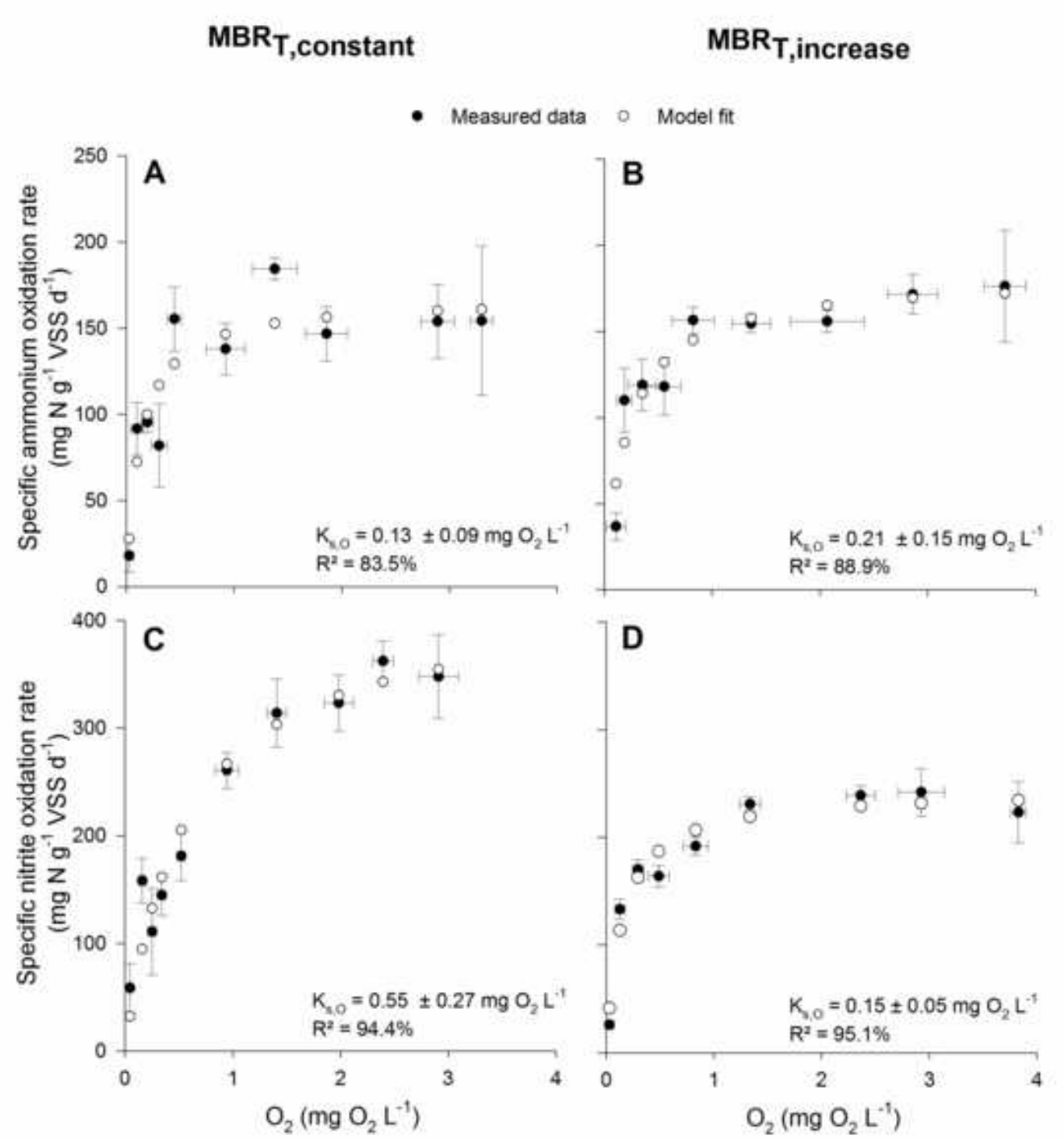

Figure 5
Click here to download high resolution image

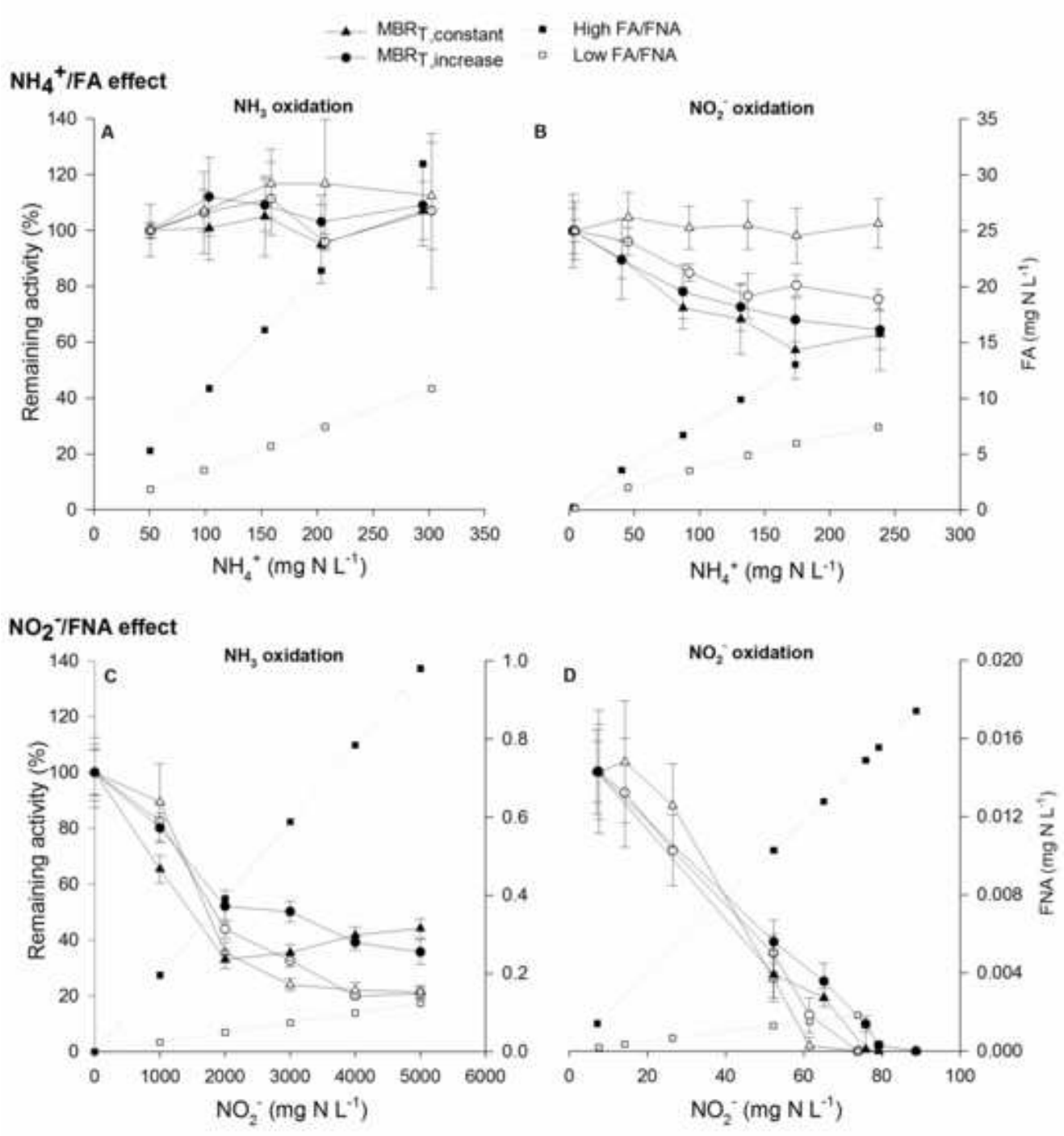

Figure 6
Click here to download high resolution image

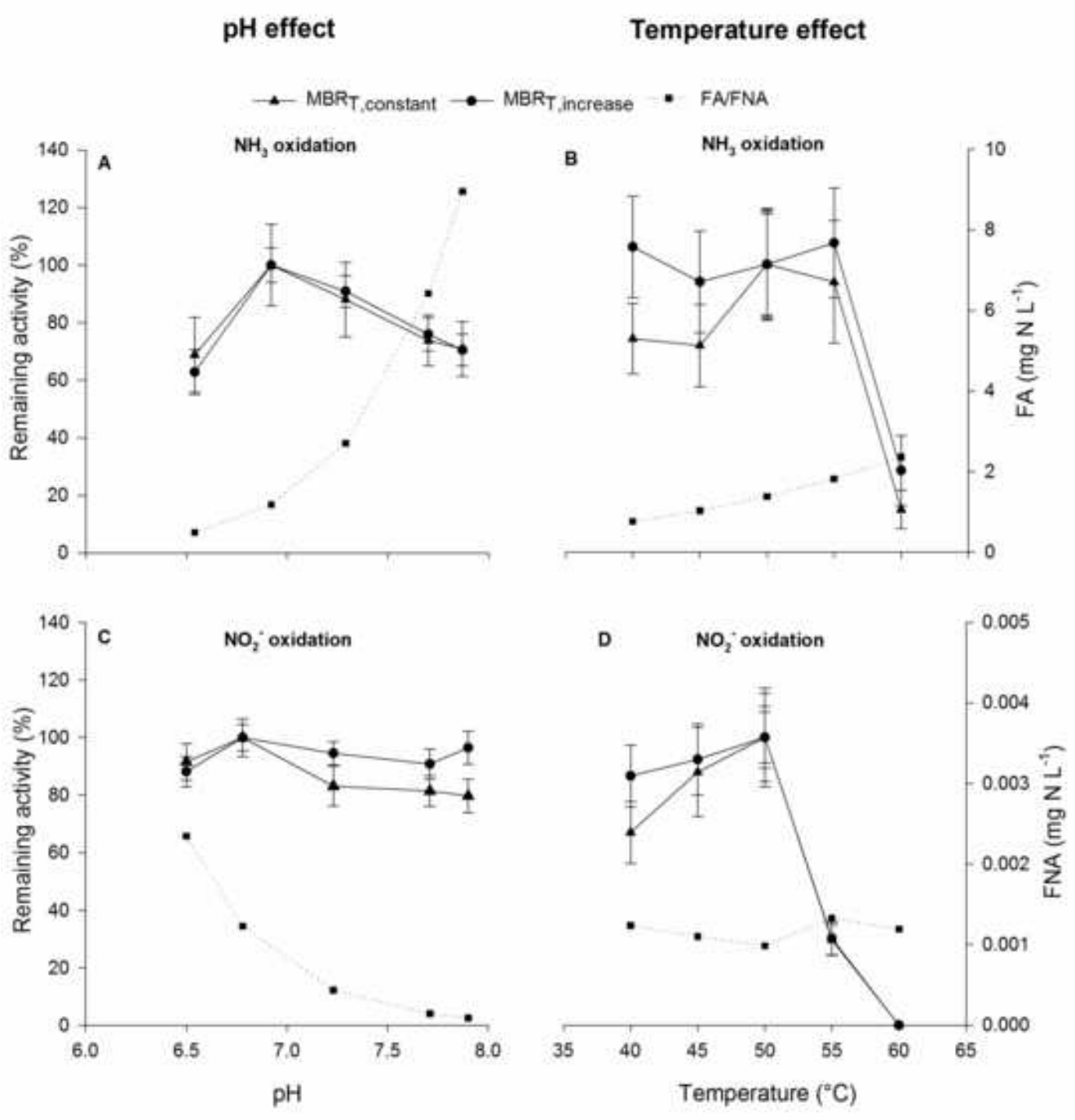

Figure 1

Click here to download high resolution image

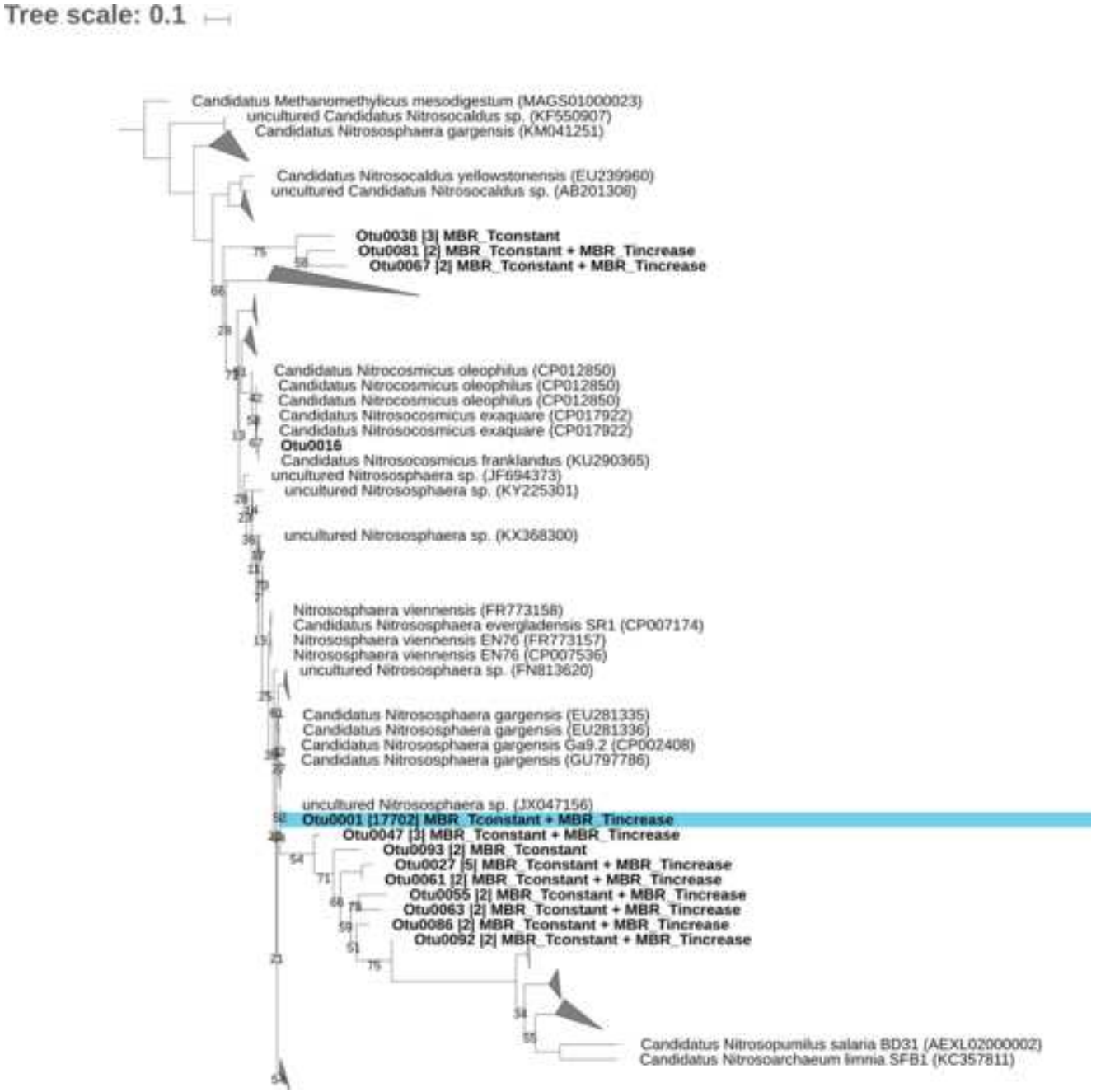

Figure 2

Click here to download high resolution image

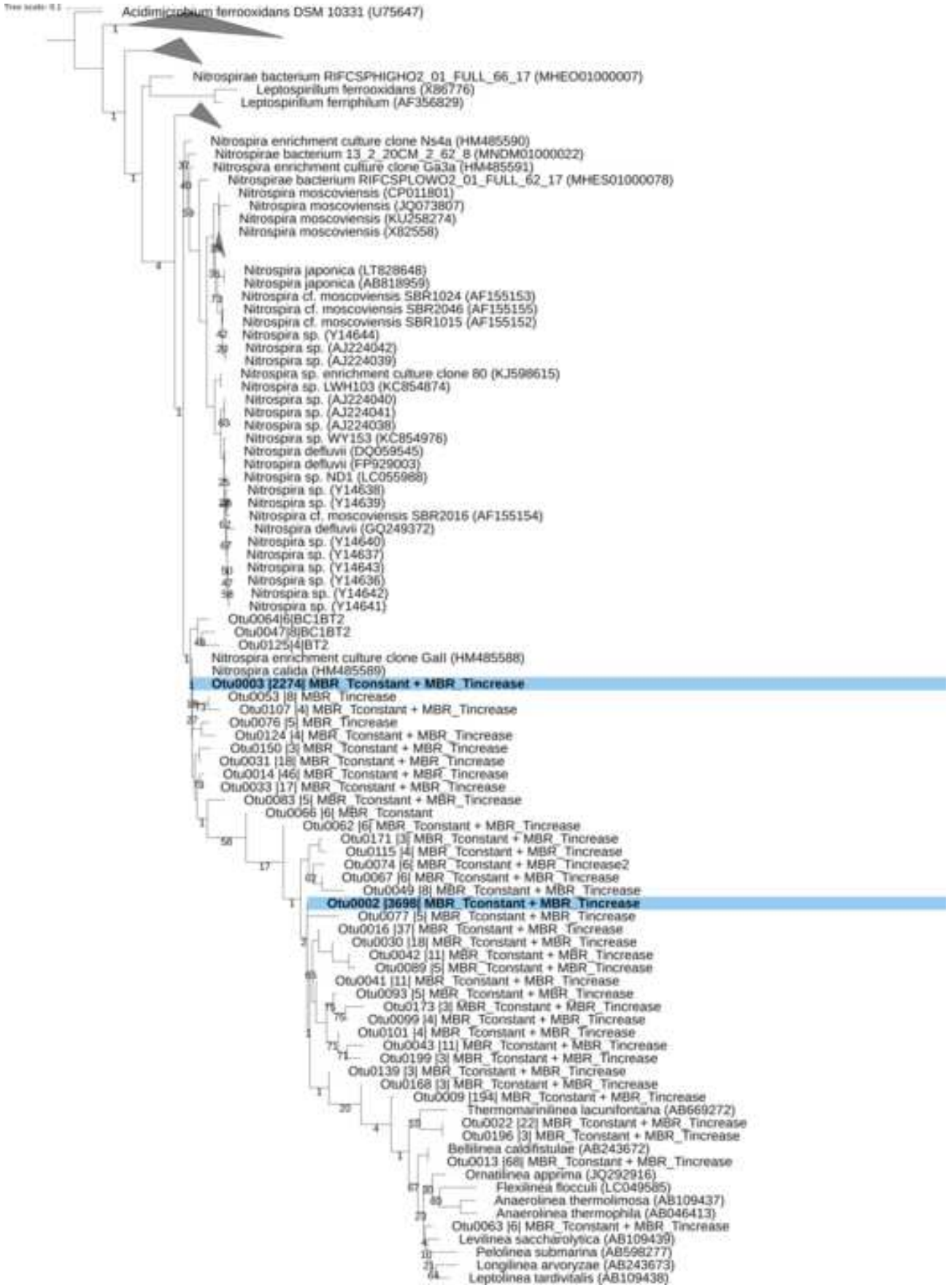

Electronic Supplementary Material (for online publication only)

Click here to download Electronic Supplementary Material (for online publication only): Supplementary material_autotrophic kin